Acta Materialia 164 (2019) 440–453

Contents lists available at ScienceDirect

Acta Materialia

journal homepage: www.elsevier.com/locate/actamat

Full length article

Dislocation absorption and transmutation at $\{10\bar{1}2\}$ twin boundaries in deformation of magnesium

Peng Chen [a, b], Fangxi Wang [a, b], Bin Li [a, b, *]

[a] Department of Chemical and Materials Engineering, University of Nevada, Reno, USA
[b] Nevada Institute for Sustainability, University of Nevada, Reno, USA

ARTICLE INFO

Article history:
Received 8 September 2018
Received in revised form
25 October 2018
Accepted 31 October 2018
Available online 3 November 2018

Keywords:
Twinning
Dislocation
Twin-slip interaction

ABSTRACT

How matrix dislocations, i.e. basal, prismatic and pyramidal, interact with $\{10\bar{1}2\}10\bar{1}\bar{1}$ twin boundaries in hexagonal close-packed metals has been discussed extensively in the literature. However, so far no systematic investigation has been reported. In this work, we performed atomistic simulations to study interaction between matrix dislocations in pure Mg with a $\{10\bar{1}2\}$ twin boundary. Our results show that for the basal and the prismatic slip, when the Burgers vector is parallel to the zone axis of the twins, a matrix basal dislocation can be transmuted to a twin prismatic dislocation and vice versa. However, when the Burgers vector of the matrix dislocation is non-parallel to the zone axis, no transmutation occurs and the dislocation is absorbed by the twin boundary which acts as a dislocation sink. For a matrix pyramidal dislocation, the dislocation is absorbed by the twin boundary and no transmutation occurs either. It appears that if the product dislocation is a real slip system, transmutation may occur during twin-slip interaction. Otherwise the matrix dislocation will be shredded by atomic shuffling and then absorbed by the twin boundary. If the core structure of the product dislocation is complex, transmutation may not occur as well and dislocation absorption will occur. Lattice correspondence in deformation twinning was applied in explaining the interaction mechanisms. Our results can be well correlated to macroscopic experimental observations which show twin-slip interaction only contributes negligibly to work hardening in deformation of hcp metals.

1. Introduction

Dislocation slip and deformation twinning are the most important mechanisms determining the mechanical properties of crystalline materials. When a dislocation impinges on a twin boundary (TB), several scenarios may occur: (1) The dislocation may be absorbed by the TB [1,2]; (2) The dislocation transmits through the TB and then glides on a slip plane in the twin that is crystallographically equivalent to the original slip plane in the parent [3–7]. For instance, in face-centered-cubic (fcc) metals, a dislocation on a {111} slip plane may transmit through a TB and then glides on a {111} plane of the twin; (3) Dislocation may be transmuted by the TB. In this case, the matrix dislocation is transformed to a dislocation in the twin, but the slip plane is a corresponding plane of the original slip plane in the parent [5,7], which is oftentimes a crystallographically different plane than the original slip plane; (4) The dislocation slip is hindered by the TB which acts as a barrier to dislocation slip [8–10]. In cubic metals, TBs are coherent and coincident with the twinning plane, transmission of matrix dislocations into the twin is often observed and interaction mechanisms between a matrix dislocation and a TB have been investigated [4,11]. In nanostructured metals in which twinning is more favored than in coarse-grained metals [12–16], twin-slip interaction was found to be affected by the twin boundary spacing [13,14], dislocation density [15] and loading direction with respect to the twinning plane [14,16].

For hexagonal close packed (hcp) metals, unlike fcc metals in which dislocation slip dominates plastic deformation under conventional conditions in terms of temperature and strain rate, profuse and multiple twinning modes can be activated [17,18], with $\{10\bar{1}2\}10\bar{1}\bar{1}$ mode being the most commonly observed one [19–23]. How this twinning mode interacts with matrix

* Corresponding author. Department of Chemical and Materials Engineering, University of Nevada, Reno, USA.
E-mail address: binl@unr.edu (B. Li).

https://doi.org/10.1016/j.actamat.2018.10.064
1359-6454/

dislocations has been an important subject in the studies of deformation behavior of hcp metals, especially in recent years when magnesium (Mg) and its alloys have been deemed as promising lightweight structural materials for engineering applications.

Twin-slip interaction in Mg and other hcp metals has been studied in numerous reports [24–31], and how twin-slip interaction affects the hardening behavior has been discussed extensively [32–35]. Generally it has been believed that twin-slip interaction contributes to hardening in three ways: (1) TBs act as obstacles to dislocation slip [36] and preexisting dislocations in matrix may impede twin nucleation and twin growth [37]; (2) Dynamic Hall-Petch effect [34,38,39]. Twin laths divide the parent grains into smaller grains, reducing the mean free path for dislocation interaction; (3) Dislocation transmutation [40–42]. This mechanism was proposed in light of the Basinski effect [43] which was observed in fcc copper. Basinski et al. [43] found that the hardness of twins was higher than that of the matrix and this increase in hardness was ascribed to transformation of mobile dislocations to immobile dislocations in the twin. However, the contribution of twin-slip interaction to work hardening was questioned by a number of researchers. Capolungo et al. [44] showed that the preexisting dislocations in the matrix have almost no barrier effect on migration of $\{10\bar{1}2\}$ TBs. Hiura et al. [45] performed nano-indentation measurements and showed that the hardness difference between the twin and the surround matrix is insignificantly small in single crystal Mg. Kalidindi et al. [34] showed that the contribution of $\{10\bar{1}2\}$ twinning to hardening in AZ31B alloy is very limited, only about 0.03G (G is the shear modulus) compared to the peak strain hardening rate (~0.3G). More recently, Chen et al. [46] used pre-straining to investigate how matrix dislocations affect $\{10\bar{1}2\}$ twinning and the hardening behavior of an AZ31 extruded Mg alloy. Their results showed that, even with a pre-strain as high as 10%, the stress-strain curve presents little difference from that of zero pre-strain. These results indicate that twin-slip interaction through the Basinski mechanism and dynamic Hall-Petch effect only contributes negligibly to work hardening in Mg and Mg alloys.

It is worth noting that the twinning mechanisms in fcc metals and hcp metals are significantly even fundamentally different. In twinning of fcc metals, the twinning plane is exactly the slip plane of matrix dislocation. Both are the {111} close-packed plane and the TBs are always coherent. But for $\{10\bar{1}2\}$ twinning in hcp metals, this twinning plane is not a slip plane of any matrix dislocation. More importantly, $\{10\bar{1}2\}$ TBs are always incoherent in experimental observations and in simulations [47–50] and can hugely depart from the theoretical twinning plane [51], and the misorientation angle can vary over a wide range of values [52]. These non-classical characteristics of $\{10\bar{1}2\}$ twinning mode must be taken into consideration when twin-slip interaction is studied and discussed. More complex in twin-slip interaction in hcp metals is multiple slip systems, i.e. basal, prismatic [53,54] and pyramidal slip systems [55,56], can be activated. Interactions between $\{10\bar{1}2\}$ TBs and these different slip systems have to be investigated such that a definitive conclusion can be reached. So far, how these dislocations interact with $\{10\bar{1}2\}$ TBs and how the interaction influences macroscopic mechanical behavior of Mg alloys remains unclear, and no systematic investigation on this important issue has been reported.

The purpose of this work is to conduct atomistic simulations on how matrix dislocations in pure Mg interact with a $\{10\bar{1}2\}$ TB. The dislocations considered include basal, prismatic and pyramidal dislocations. The Burgers vectors of these dislocations are either parallel or non-parallel to the zone axis of the twins. The results obtained provide a much deeper insight on the mechanical behavior of Mg and other hcp metals.

2. Method

The embedded atom method (EAM) potential [57,58] for Mg-Al binary system was used in this work. This EAM potential was well developed by Liu et al. [59], and have been used in numerous atomistic simulations of deformation behavior of Mg and Mg-Al alloys [47,49,54,55,60].

Three scenarios of $\{10\bar{1}2\}$ twin/dislocation interactions are simulated, respectively: (1) a TB migrates and interacts with a stationary matrix dislocation; (2) a mobile matrix dislocation glides and interacts with a stationary TB; (3) a mobile matrix dislocation interacts with a migrating TB, i.e. both the matrix dislocation and the TB are mobile. In these simulations, two crystals that satisfy the $\{10\bar{1}2\}$ twin relationship were constructed and then a matrix dislocation was introduced into the parent by either artificially constructing a dislocation or deforming the system via applying an external strain.

Three types of dislocations were introduced into the system: (0002) basal, $\{10\bar{1}0\}$ prismatic and $\{10\bar{1}1\}$ pyramidal. No $\{11\bar{2}2\}$ pyramidal dislocations can be activated with the interatomic potential developed by Liu et al. [59]. For the basal and the prismatic dislocations, their Burgers vectors are all $\langle a\rangle = \left\langle 11\bar{2}0\right\rangle$ type, but two different scenarios need to be considered: (1) the Burgers vector is parallel to the zone axis of the twins; (2) the Burgers vector is not parallel to the zone axis of the twins, i.e. the Burgers vector of basal dislocation makes a 60° angle with the zone axis. For the pyramidal dislocations, the Burgers vector of these dislocations are always not parallel to the zone axis. Details of the initial structure of each scenario are shown below.

For each simulation, the system was relaxed before an external tensile strain was applied. The tensile strain was generated by moving the fixed surface atoms at a constant displacement rate of 0.01 nm per ps. The temperature was maintained at 100 K during simulation. Free surfaces were applied to all three dimensions. All simulations were run for 1000,000 timesteps and data was collected every 0.5 ps. The visualization tool Ovito [61] was used to analyze the simulation results.

3. Results

To visualize the structural evolution during simulation, common neighbor analysis (CNA) [62] was performed to distinguish the structures of dislocations, stacking faults (SF) and TB. 2D cross-sectional views and 3D views are provided to analyze the structural evolution.

3.1. Interaction between a $\{10\bar{1}2\}$ TB and a basal dislocation

3.1.1. The Burgers vector is parallel to the zone axis

Fig. 1a shows the initial configuration for simulating the interaction between a stationary matrix basal dislocation and a mobile twin boundary (TB), which is a 2D cross-sectional view. The two crystals have a misorientaion of $90°1\bar{2}10$, i.e. the TB is a basal/prismatic interface. In simulations and experiments, the $90°\left\langle 1\bar{2}10\right\rangle$ twin relationship has been extensively observed [47,50,51], although the theoretical misorientation is $86.3°\left\langle 1\bar{2}10\right\rangle$. A tensile load was applied along the [0002] of the parent. An edge basal dislocation with a Burgers vector of $\frac{1}{3}[1\bar{2}10]$ was pre-constructed inside the parent by removing a half-plane of atoms. The half plane contains two columns of atoms on the $\{1\bar{2}10\}$ planes. The Burgers vector of the created edge dislocation is parallel to the zone axis. Then the system was fully relaxed. The two ends of the dislocation are terminated at the free surfaces. A 3D view of the

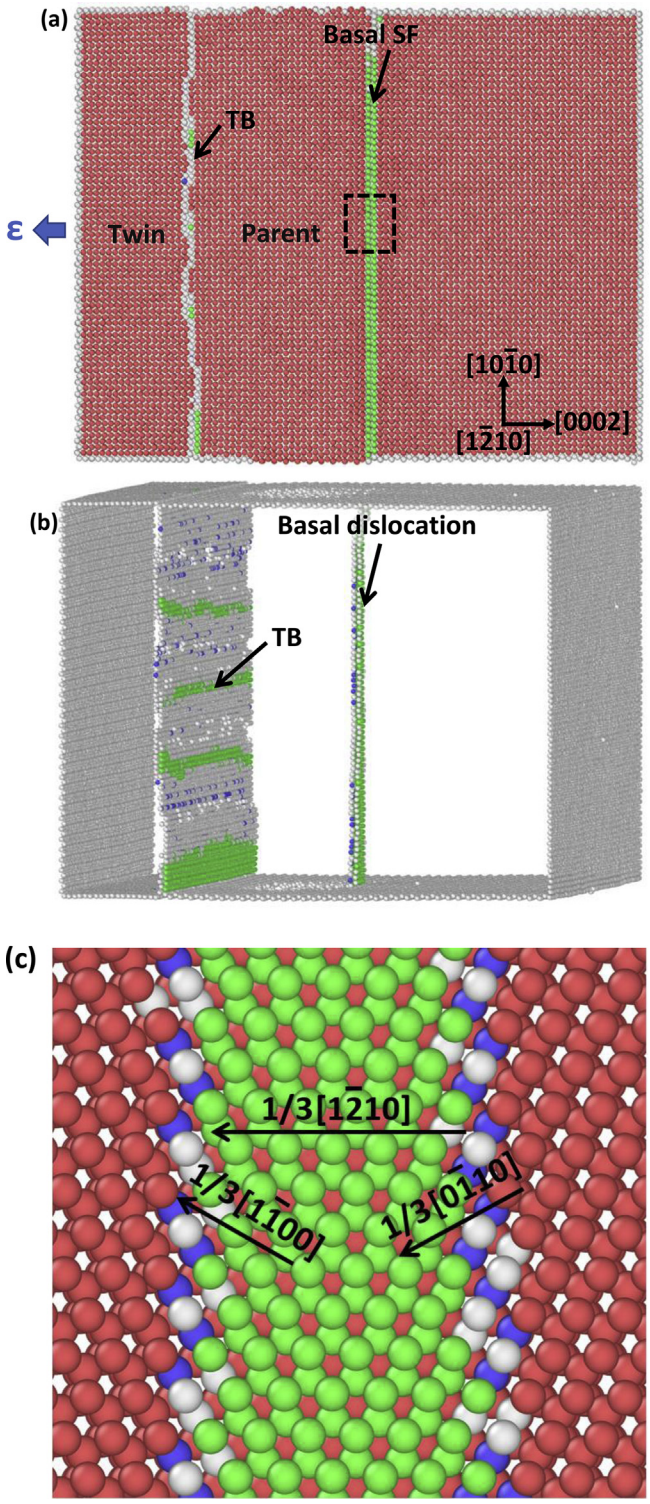

Fig. 1. (a) Initial configuration for simulating interaction between a matrix basal dislocation and a twin boundary (TB). The two crystals have a misorientaion of 90°[1$\bar{2}$10], i.e. the TB is a basal/prismatic interface. A tensile load was applied along the [0002] of the parent. Atoms inside the black box were selected for computing the interaction energy. (b) 3D view of the TB and the basal dislocation. Atoms in perfect hcp lattice are removed. (c) When viewed along the *c*-axis of the parent, the Shockley partial dislocations (in white and blue) and the basal SF (in green) can be seen. The Burgers vector of the basal dislocation is parallel to the zone axis [1$\bar{2}$10]. The width of the basal SF is ~2.0 nm. (For interpretation of the references to color in this figure legend, the reader is referred to the Web version of this article.)

TB and the basal dislocation are shown in Fig. 1b. In this plot, atoms in perfect hcp structure are removed such that only those atoms at the free surfaces, the partial dislocations, the SF and the TB are shown. When viewed along the *c*-axis of the parent, the Shockley partial dislocations (in white and blue) and the basal SF (in green) can be readily seen (Fig. 1c). The width of the basal SF is ~2.0 nm. The dissociation of the basal dislocation can be described as:

$$\frac{1}{3}\left[1\bar{2}10\right] = \frac{1}{3}\left[1\bar{1}00\right] + SF + \frac{1}{3}\left[0\bar{1}10\right] \quad (1)$$

Fig. 2 illustrates the interaction between the basal dislocation and the TB. Under the external tensile strain, the TB starts migrating toward the parent (Fig. 2a). As shown in the top portion of the TB, when the TB approaches and interacts with the basal dislocation, the original basal dislocation on the parent basal plane now becomes a dislocation on the twin prismatic plane and the color of the atoms changes from green to white. Notably, the dislocation lines in the parent and in the twin are parallel. As the strain increases, the TB continues traversing through the parent. Eventually, the TB entirely passes and transforms the basal dislocation to the

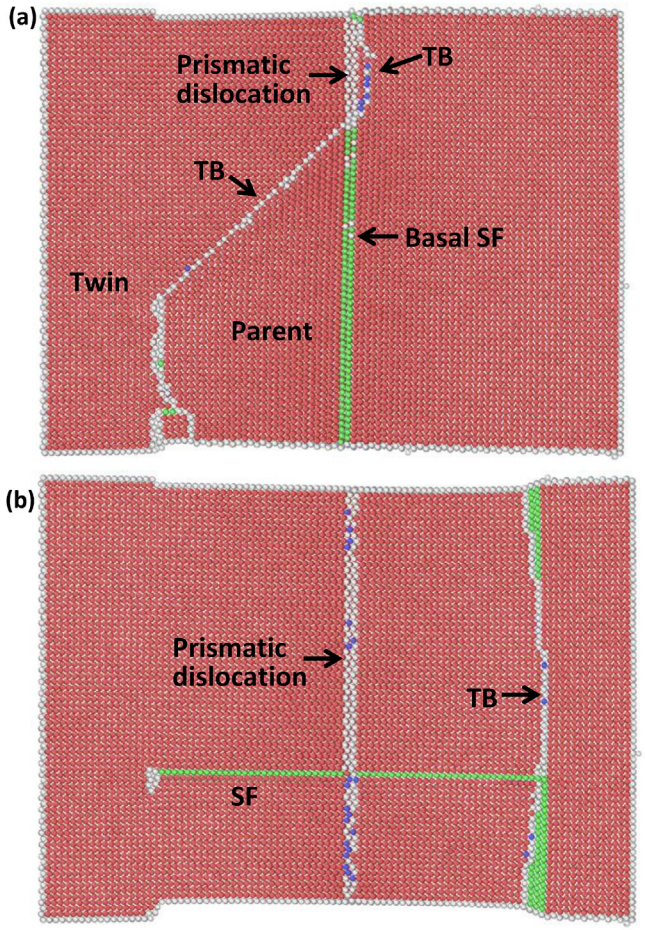

Fig. 2. Interaction between the basal dislocation and the twin boundary (TB). (a) The TB approaches and interacts with the basal dislocation under the tensile strain. The top potion of the TB passes the SF and transforms the basal dislocation into a prismatic dislocation. (b) The TB entirely passes and transforms the basal dislocation to a prismatic dislocation. A basal stacking fault, represented by a single layer green atoms, is created inside the twin as a result of TB migration. (For interpretation of the references to color in this figure legend, the reader is referred to the Web version of this article.)

prismatic dislocation (Fig. 2b). During straining, the basal dislocation remains still because the Schmid factor equals zero. After the TB transforms the basal dislocation to the prismatic dislocation, the prismatic dislocation also remains still, i.e. immobile. Inside the twin, another basal SF is generated. This basal SF is shown in a single layer of green atoms, different from the basal SF of two-layer green atoms (cf. Fig. 2a). With one end anchored at the TB, this SF grows as the TB migrates, thus, the width of this SF can be much wider than the equilibrium width (~2.0 nm, Fig. 1c). This new basal SF is called "partial stacking faults" [49,63,64] and has nothing to do with the activities of partial dislocations.

To identify the Burgers vector of the prismatic dislocation inside the twin, Burgers vector analysis was performed. In Fig. 3a, a Burgers circuit was drawn surrounding the basal dislocation in the matrix before straining. It can be readily seen that the Burgers vector equals $\frac{1}{3}[1\bar{2}10]$ which is parallel to the zone axis. After the TB traverses through, the parent basal planes are transformed to the twin prismatic planes. Accordingly, the dislocation line now lies in the prismatic plane with a Burgers vector of $\frac{1}{3}[1\bar{2}10]$. This indicates that the TB-dislocation interaction does not change the Burgers vector in this particular case. These Burgers vector analyses were also confirmed by the dislocation analysis tool in Ovito [65]. This transmutation can be described as:

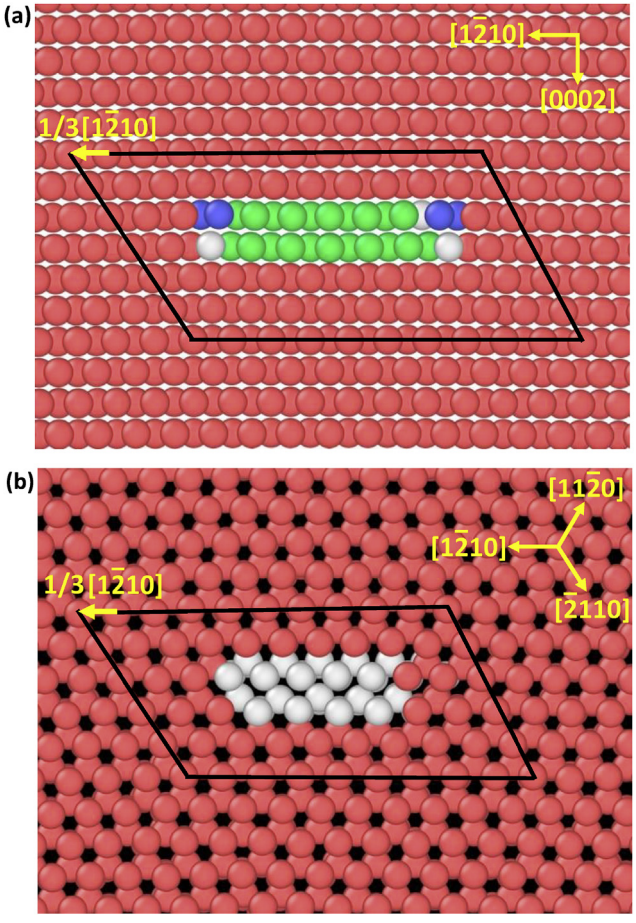

Fig. 3. Burgers vector analysis for the dislocations. (a) Before the interaction. The Burgers vector of the matrix basal dislocation is determined as $\frac{1}{3}[1\bar{2}10]$ which is parallel to the zone axis of the twins. (b) After the interaction. It can be seen that the parent basal planes are transformed to the twin prismatic planes. Accordingly, the original basal dislocation is transformed to a prismatic dislocation and the Burgers vector is still $\frac{1}{3}[1\bar{2}10]$, indicating the interaction does not change the Burgers vector.

$$\frac{1}{3}\left[1\bar{2}10\right]_{(0002)|Parent} \rightarrow \frac{1}{3}\left[1\bar{2}10\right]_{(10\bar{1}0)|Twin} \quad (2)$$

To quantitatively evaluate the energy barrier for dislocation transmutation in this scenario, we computed potential energy of the atoms inside the black box (Fig. 1a) and plotted the evolution of the energy during deformation. The result is shown in Fig. 4. The box contains a portion of the basal dislocation line with 18940 atoms. As the deformation continues, the energy gradually increases due to the elastic deformation. As the deformation further proceeds, at 850 ps, a sharp increase of the energy occurs, corresponding to the occurrence of the interaction between the TB and matrix basal dislocation (Fig. 2a). After the matrix basal dislocation is transmuted to the prismatic dislocation in the twin, the energy plummets, corresponding to the completion of the transmutation. The energy barrier of the dynamic transmutation of a matrix basal dislocation to a prismatic dislocation in the twin is ~4.2 meV/atom. Compared to the energy barrier for homogeneous $\{10\bar{1}2\}$ twin nucleation (~27 meV/atom) for Mg [66], this value for TB migration is reasonable. In nano-twinned fcc copper, Zhu et al. [12] computed the activation energy, i.e. the energy barrier for direct transmission of a $\{111\}\langle 1\bar{1}0\rangle$ dislocation through a {111} coherent TB, by using the climbing image nudged elastic band (CINEB) [67] method. A value of 670 meV/atom was obtained. Thus, the energy barrier of dislocation transmutation in fcc is two orders of magnitude higher than that in hcp Mg, indicating the twinning mechanisms are very different in these two crystal structures.

3.1.2. *The Burgers vector is not parallel to the zone axis*

To simulate the interaction between an immobile matrix basal dislocation and a mobile TB but the Burgers vector of the dislocation is not parallel to the zone axis, we used similar construction to Fig. 1a, however, we rotated the twin lattice around the [0002] of the twin by 60°. Thus, the *c*-axes of the parent and the twin remains perpendicular to each other, but the twin variant is different. The initial configuration is shown in Fig. 5. Now the Burgers vector of the basal dislocation makes 60° with the zone axis $[1\bar{2}10]$. Atoms inside the black box (a total of 23718 atoms) were selected for computing the interaction energy. The process of interaction is shown in Fig. 6. In Fig. 6a, as the TB approaches and finally impinges with the matrix basal dislocation, both the partial dislocations and the basal SF disappear, i.e. they are absorbed by the moving TB. Eventually, the basal dislocation is fully consumed as the TB sweeps through the parent (Fig. 6b). A 3D view of Fig. 6b is displayed in Fig. 6c. It can be seen that no trace of the partial dislocations and the SF is left behind after the TB entirely passes the original dislocation

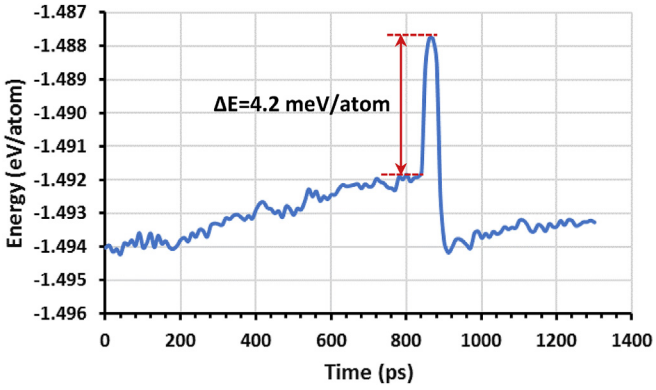

Fig. 4. Energy evolution during interaction between the TB and the basal dislocation when transmutation occurs. The energy barrier for dislocation transmutation is about 4.2 meV/atom.

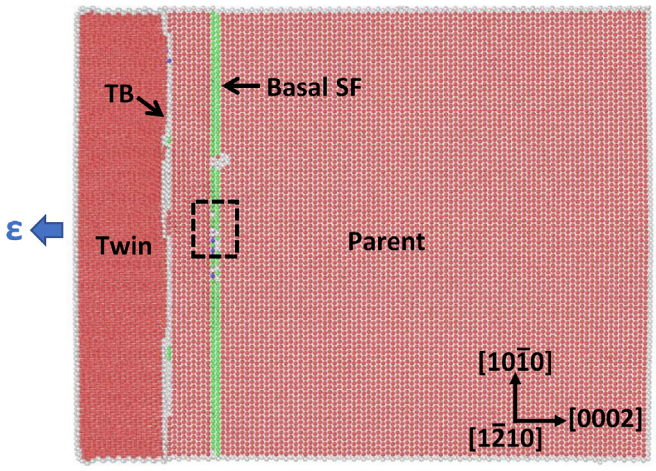

Fig. 5. Initial configuration for simulating the interaction between a matrix basal dislocation and a TB, but the Burgers vector of the basal dislocation makes 60° with the zone axis [1$\bar{2}$10]. A tensile load was applied along the [0002] of the parent. Atoms inside the black box were selected for computing the interaction energy.

line. In this scenario, the Schmid factor of the basal dislocation also equals zero, so the dislocation remains still during straining.

The energy barrier for the basal dislocation absorption by the TB is shown in Fig. 7. The energy barrier equals ~3.1 meV/atom. The energy barrier for dislocation absorption in fcc copper was ~490 meV/atom [12]. Again, the energy barrier for dislocation absorption in Mg is much lower than fcc metals.

In the following, we examine how a mobile basal dislocation interacts with an immobile TB by changing the loading direction with respect to the normal of the parent basal plane. Fig. 8 shows the initial configuration for simulating the interaction between a mobile matrix basal dislocation and an immobile $\{10\bar{1}2\}$ TB. The twin crystals have a misorientation of 86.3°[1$\bar{2}$10]. A basal dislocation was pre-constructed in the parent, but its Burgers vector is not parallel to the zone axis of the twins. The nearly coherent TB is parallel to the $\{10\bar{1}2\}$ twinning plane which is horizontal. A tensile load was applied perpendicular to the TB. In this configuration, the basal dislocation has a maximal Schmid factor and will glide toward the TB when the critical shear stress is reached. In Fig. 9, we show snapshots in time sequence to illustrate how the matrix basal dislocation glides and interacts with the TB. Fig. 9a and b shows the basal dislocation glides and approaches the TB under the external strain. In Fig. 9c, the basal dislocation impinges on the TB. Eventually, the basal dislocation is completely absorbed by the TB (Fig. 9d). At the location of impingement, the TB becomes less coherent. Obviously, no dislocation transmutation occurs in this case.

In the simulation of the interaction between a mobile matrix basal dislocation and a mobile $\{10\bar{1}2\}$ TB, we first constructed twin crystals that satisfy 86.3°[1$\bar{2}$10] twin relationship, similar to Fig. 8, but the tensile load was applied in the vertical direction with a 70° angle with the TB (Fig. 10). As shown in Fig. 11, under the tensile load, the TB migrates downward. Meanwhile, a leading Shockley partial dislocation is nucleated on the free surface and glides toward the moving TB. The boxed region in Fig. 11 is further analyzed in Fig. 12 in time sequence. In Fig. 12a, the leading partial is gliding toward the TB, and then impinge on the TB (Fig. 12b). The trailing partial is falling behind and a wide basal SF can be seen. During interaction, the leading partial is absorbed by the TB. Meanwhile, the trailing partial catches up and eliminate SF (Fig. 12c). Eventually, the trailing partial also impinges on the TB. As a result, the two partials and the SF completely disappear and are absorbed by the TB (Fig. 12d). Obviously, no dislocation transmutation occurs either.

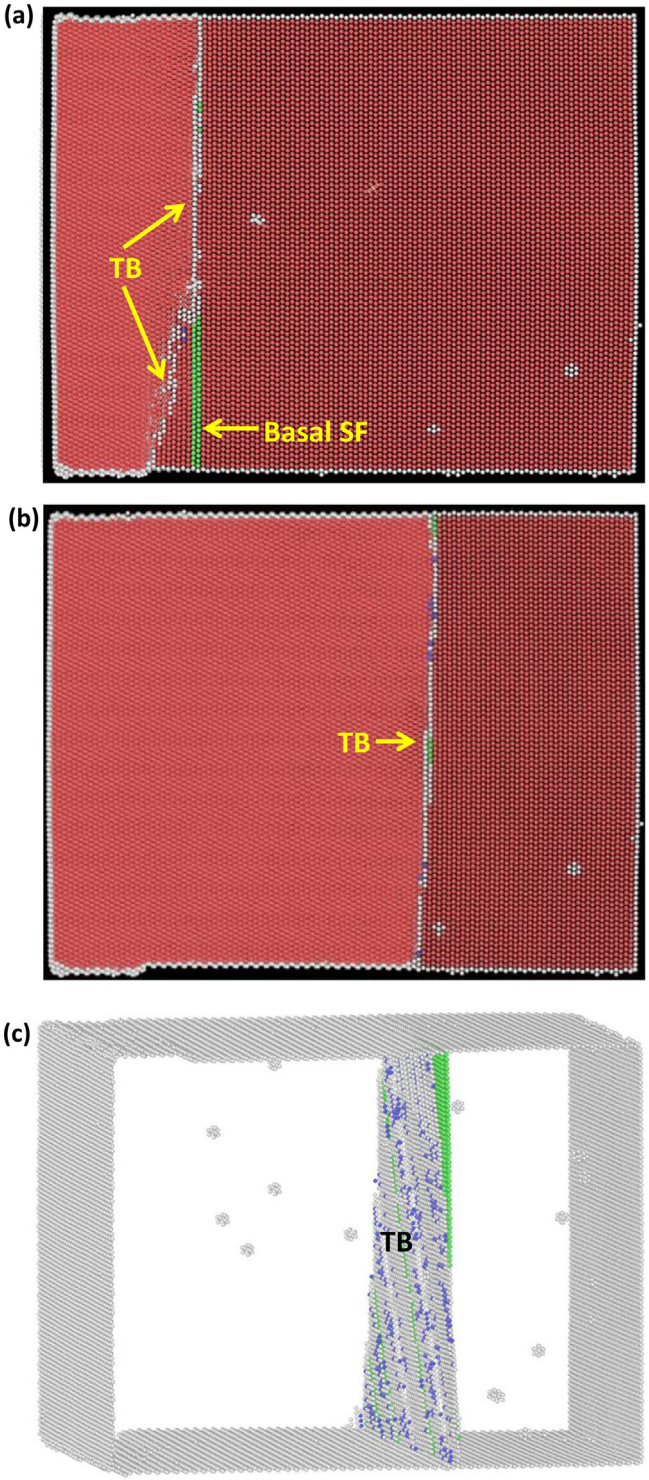

Fig. 6. Absorption of the basal dislocation by the moving twin boundary (TB) when the Burgers vector is not along the zone axis of the twins. (a) As the TB impinges with the basal dislocation, the partial dislocations and the SF disappear. (b) The matrix basal dislocation is fully consumed by the TB. (c) 3D view of (b). No trace of the partial dislocations and the SF is left behind as the TB sweeps through.

3.2. Interaction between a $\{10\bar{1}2\}$ TB and a matrix prismatic dislocation

3.2.1. The Burgers vector is parallel to the zone axis

Similar to the simulations of interaction between a matrix basal

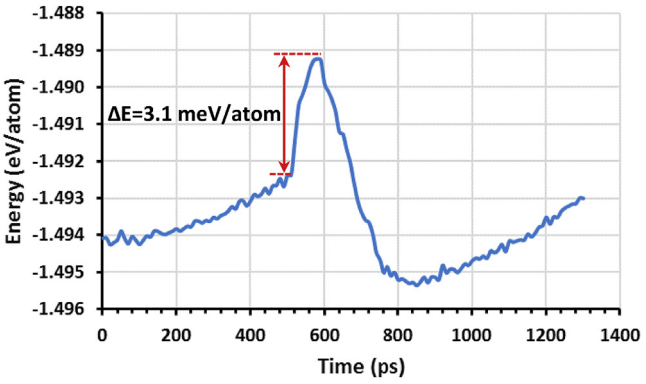

Fig. 7. The energy evolution during interaction between the TB and the basal dislocation when absorption occurs. The energy barrier for dislocation absorption is about 3.1 meV/atom.

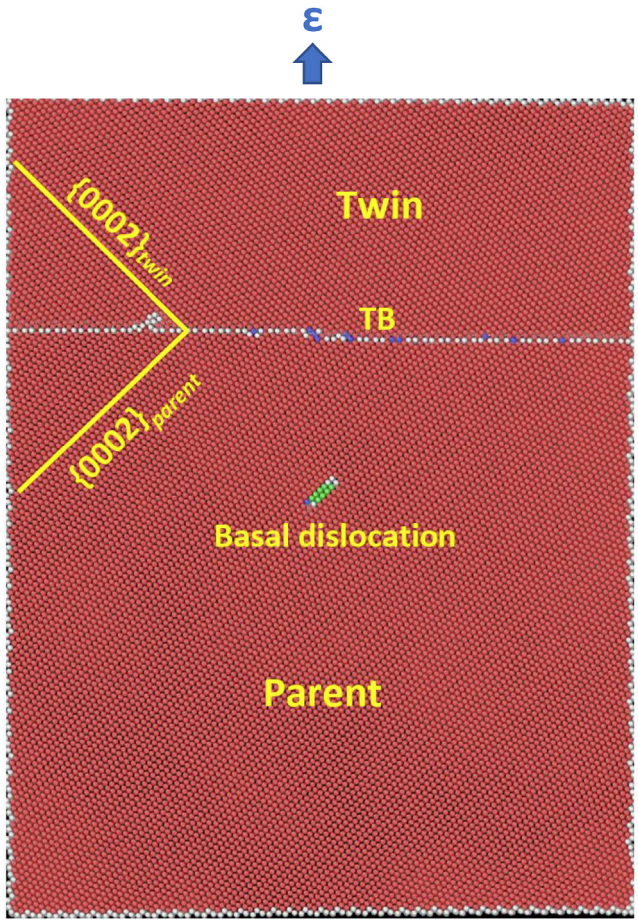

Fig. 8. Initial configuration for simulating interaction between a mobile matrix basal dislocation and an immobile $\{10\bar{1}2\}$ twin boundary (TB). The two crystals have a misorientaion of 86.3°$[1\bar{2}10]$. A basal dislocation was preconstructed in the parent. A tensile load was applied perpendicular to the TB.

dislocation and a $\{10\bar{1}2\}$ TB, we performed simulations of interaction between a matrix prismatic dislocation and a $\{10\bar{1}2\}$ TB. Two scenarios were considered: (1) the Burgers vector of the matrix prismatic dislocation is parallel to the zone axis of the twins; (2) the Burgers vector of the matrix prismatic dislocation is not parallel to the zone axis of the twins.

Fig. 13 shows the initial configuration for simulating interaction between a matrix prismatic dislocation and a TB with the Burgers vector being parallel to the zone axis $[1\bar{2}10]$. Similar to the construction of an edge basal dislocation, an edge prismatic dislocation was created in the parent by removing a half-plane of atoms. Then the system was fully relaxed. It can be seen that the prismatic dislocation is slightly dissociated. A tensile load was applied along the [0002] of the parent. A 3D view of the TB and the prismatic dislocation is displayed in Fig. 13b in which the atoms of hcp structure are removed. It can be seen that one end of the prismatic dislocation is terminated at the TB and the other at the free surface.

Under the tensile strain, the TB migrates and interacts with the prismatic dislocation (Fig. 14a). As the TB is interacting with the prismatic dislocation, left behind is a new dislocation on the basal plane in the twin. The two dislocations connect at the TB. The basal dislocation in the twin is slightly dissociated and an SF (in green) is bounded by the two partial dislocations. As the TB traverses through the parent, the matrix prismatic dislocation is gradually transformed into a basal dislocation in the twin.

We performed Burgers vector analysis for the TB-prismatic interaction in Fig. 14 and the results are shown in Fig. 15. The dislocation analysis tool in Ovito [65] was also used to confirm the analysis. Fig. 15a shows the Burgers vector of the prismatic dislocation before interacting with the moving TB. The Burgers vector of the matrix prismatic dislocation can be identified as $1/3[1\bar{2}10]$. After the TB interacts and transforms the matrix prismatic dislocation into basal dislocation in the twin, the Burgers vector remains parallel to the zone axis. This interaction can be described as:

$$\frac{1}{3}\left[1\bar{2}10\right]_{(10\bar{1}0)|Parent} \rightarrow \frac{1}{3}\left[1\bar{2}10\right]_{(0002)|Twin} \rightarrow \frac{1}{3}\left[1\bar{1}00\right] + SF + \frac{1}{3}\left[0\bar{1}10\right] \tag{3}$$

3.2.2. The Burgers vector is not parallel to the zone axis

The initial configuration of the simulation of the interaction between a $\{10\bar{1}2\}$ TB and a matrix prismatic dislocation that has a Burgers vector making 60° with the zone axis $[1\bar{2}10]$ is shown in Fig. 16. This configuration is similar to that in Fig. 13a, but the twin is rotated around the c-axis of the parent by 60°. The process of interaction is shown in Fig. 17. It can be seen from Fig. 17a that, as the TB migrates into the parent and interacts with the matrix prismatic dislocation, the prismatic dislocation is being absorbed by the TB and no trace of the prismatic dislocation is left behind the TB inside the twin. This is further revealed in the 3D view (Fig. 17b). Obviously, no dislocation transmutation occurs in this case, which is similar to the case in which the Burgers vector of the matrix basal dislocation is not parallel to the zone axis of the twins.

3.3. Interaction between a $\{10\bar{1}1\}$ pyramidal dislocation and a $\{10\bar{1}2\}$ TB

In the literature, two types of pyramidal slip systems in Mg and Mg alloys were reported: $\left\{11\bar{2}2\right\}\left\langle11\bar{2}3\right\rangle$ and $\left\{10\bar{1}1\right\}\left\langle11\bar{2}3\right\rangle$ [55,56,68]. Possible dissociation of these pyramidal dislocations were investigated by using atomistic simulations [55,68,69], however, the obtained results have not been confirmed by experiments. Experimentally it is very difficult to definitively determine the slip plane and the Burgers vectors of the partial dislocations of these pyramidal slip systems. To overcome these uncertainties, we did not pre-construct a pyramidal dislocation in the system, instead,

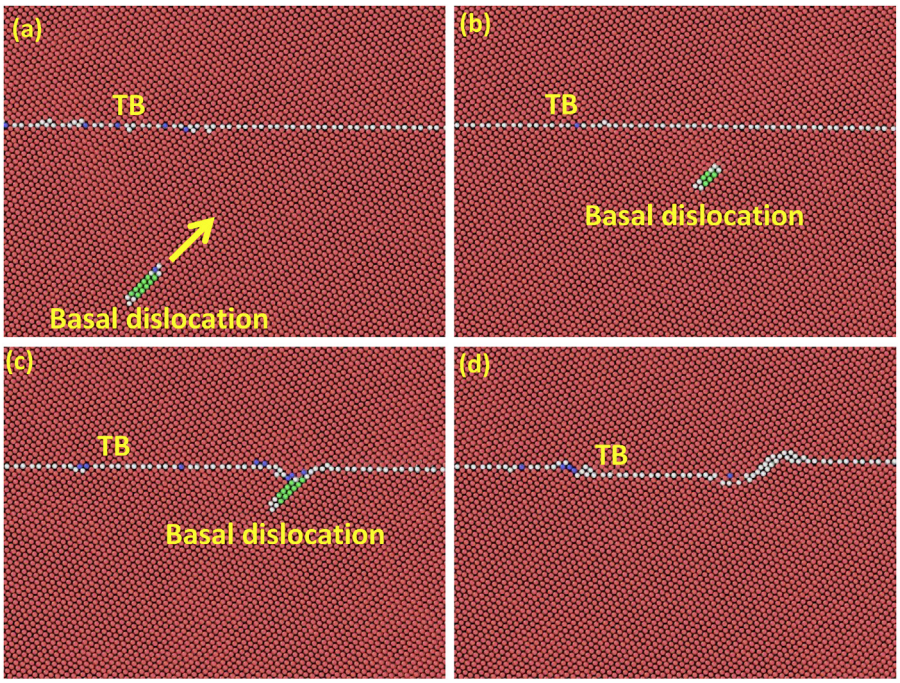

Fig. 9. Snapshots in time sequence showing the matrix basal dislocation glides and interacts with the TB. (a) The basal dislocation glides toward the TB. (b) The basal dislocation approaches the TB. (c) The basal dislocation impinges on the TB. (d) The basal dislocation is completely absorbed by the TB. No transmutation occurs in this case.

we pre-planted a nano-sized crack in the parent to facilitate the pyramidal dislocation nucleation during straining. As such, the TB will migrate and interact with whatever pyramidal dislocations that are nucleated by the deformation. Fig. 18 shows the initial configuration for simulating the interaction between a TB and a pyramidal dislocation. A nano-crack is pre-planted on the bottom surface of the parent to facilitate nucleation of pyramidal dislocations. A tensile load was applied along the [0002] of the parent.

The evolution of the system under the external tensile strain is shown in Fig. 19. We present snapshots of the interaction process in time sequence. In Fig. 19a, as the tensile strain increases, the TB migrates toward the parent. Meanwhile, two leading partial dislocations nucleate from the nano-crack. One partial glides toward the TB and the other away from the TB. The slip planes can be identified as $\{10\bar{1}1\}$, i.e. the first order pyramidal. Each partial leaves an SF behind its wake. The trailing partials are not nucleated yet. Eventually, the left leading partial impinges on the TB and interacts with the TB. At the location of impingement, the TB becomes more incoherent in the sense that two small basal/prismatic and prismatic/basal interfaces are created (Fig. 19b). As the TB continues gliding forward, a basal SF is created with one end being connected to the impinging point and the other end being anchored at the moving TB. Again, this basal SF is shown in a single layer of atoms that are colored in green in the common neighbor analysis. Thus, the basal SFs are partial stacking faults (PSFs) that have nothing to do with the activities of partial dislocations [63,64]. This implies that during the interaction between the leading partial on the $\{10\bar{1}1\}$ pyramidal plane and the TB, the leading partial is absorbed by the moving TB. However, the impingement disrupts the structure of the TB and hence the lattice transformation, causing some atoms to shuffle to the faulted positions of the basal plane and producing the PSFs on the twin basal planes that appear as a single layer of green atoms (Fig. 19c). As the TB keeps gliding forward and interacting with the pyramidal SF, more PSFs are created emanating from the faulted $\{10\bar{1}1\}$ plane. Further straining causes more parent lattice transformed to the twin lattice (Fig. 19d). Now the left leading partial is totally absorbed with multiple PSFs left behind. The TB continues migrating forward and now interacting with right pyramidal SF. Finally, both pyramidal SFs are consumed by the moving TB (Fig. 19e), and more PSFs are created as a result of the interaction.

The Burgers vector of the leading partial on the $\{10\bar{1}1\}$ plane is analyzed in Fig. 20a. It can be seen that the Burgers vector equals $1/4[10\bar{1}\bar{2}]$. This Burgers vector has both $\langle a\rangle$ and $\langle c\rangle$ components. A 3D view of the pyramidal SFs is shown in Fig. 20b.

4. Analysis and discussion

4.1. Basinski effect and dislocation transmutation

The concept that a dislocation in the matrix can be converted to a dislocation in the twin came from the fact there is a strict one-to-one lattice correspondence between the parent and the twin [17]. This concept was well explained by Christian in his posthumous book [70]. It follows that a crystallographic plane of the matrix must be converted to a corresponding plane of the twin by the lattice transformation. In the classical theory of deformation twinning, the lattice transformation from parent to twin is accomplished by a homogeneous simple shear which carries all or a portion of the atoms in the parent to the twin lattice. This simple shear is mediated by the gliding of twinning dislocation on the first invariant plane (K_1) along the shear direction (η_1). In the case of fcc metals, twinning occurs by a simple shear on the close-packed planes of $(1\bar{1}1)$ along the $\langle 121\rangle$ direction mediated by Shockley partial dislocations. The transformation of parent lattice to the twin lattice was described by Basinski et al. [43] with the following transformation relations:

$$V_T = CV_M \tag{4}$$

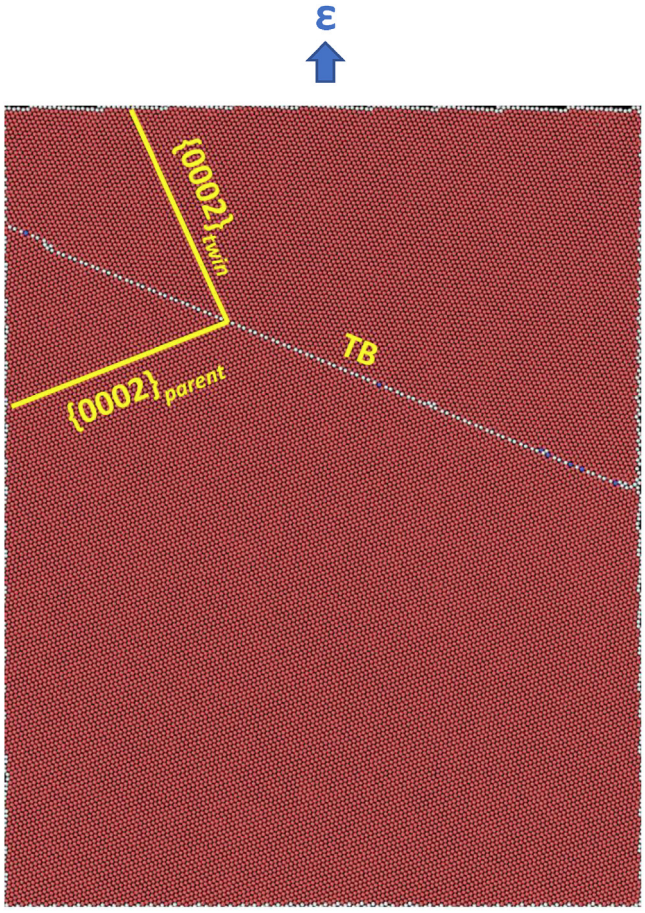

Fig. 10. Initial configuration for simulating interaction between a mobile matrix basal dislocation and a mobile $\{10\bar{1}2\}$ TB. A tensile load was applied in the vertical direction with a 70° angle with the TB such that both the dislocation and the TB are mobile.

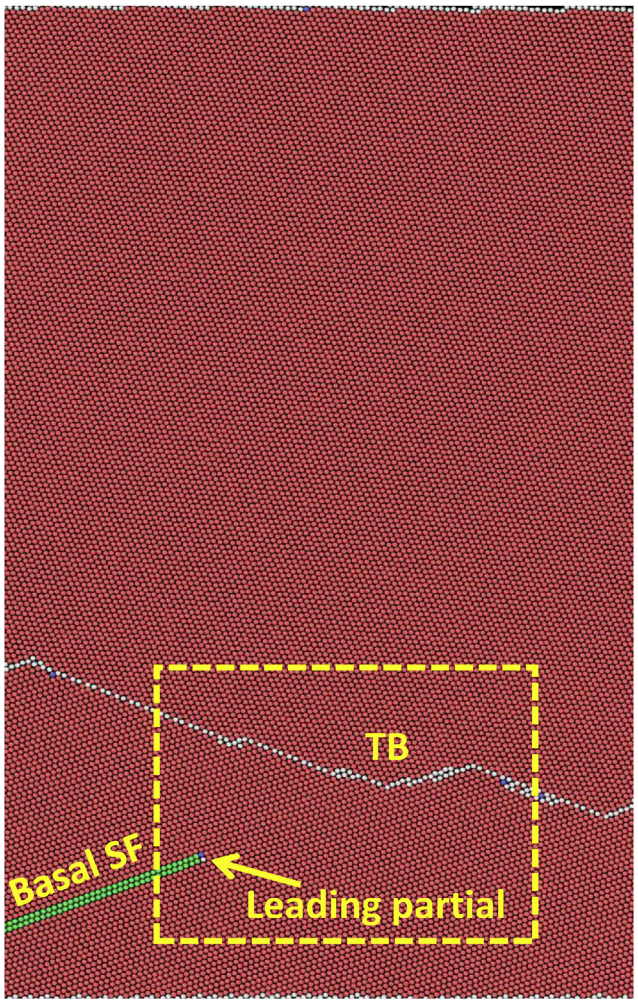

Fig. 11. Under the tensile load, the TB migrates downward. Meanwhile, a Shockley partial dislocation nucleates and glides toward the moving TB. The boxed region is analyzed in Fig. 12.

$$n_T = n_M C^{-1} \tag{5}$$

where V_M and n_M are any vector or any plane normal in the matrix lattice, V_T and n_T represent the corresponding vector or plane normal after the slip system is transformed into the twin, C is the correspondence matrix.

In light of the work by Basinski and Christian [17,43], Niewczas [71] considered all four major twinning mode in hcp metals including Mg and developed the corresponding matrices for these twinning modes. Specifically for Mg, the following lattice correspondences (Table 1) between planes/directions in the parent and planes/directions in the twin were obtained for $\left\{10\bar{1}2\right\}\left\langle 10\bar{1}\bar{1}\right\rangle$ twinning mode [71]:

Table 1 only lists the basal and the prismatic slip systems calculated by Niewczas [71]. It can be seen that, for the three basal slip systems, transmutation only occurs for one of them in our simulations and in this particular case the Burgers vector is parallel to the zone axis of the twins. As shown in Figs. 2 and 3, the Burgers vector remains unchanged before and after transmutation. Because the parent basal and the twin prismatic are reciprocal corresponding planes in $\left\{10\bar{1}2\right\}\left\langle 10\bar{1}1\right\rangle$ twinning, it is understandable that a parent prismatic dislocation will be transmuted to a twin basal dislocation when the Burgers vector is parallel to the zone axis of the twins. For other parent basal and prismatic dislocations with Burgers vectors non-parallel to the zone axis of the twins, transmutation did not occur although mathematically such transmutations were predicted. For $\left\{10\bar{1}1\right\}\left\langle 11\bar{2}\bar{3}\right\rangle$ pyramidal slip systems in the parent, none of these Burgers vectors is parallel to the zone axis of the twins, thus, no transmutation occurs. According to our simulation results, when transmutation does not occur, the dislocations are simply annihilated or absorbed by the TB which acts as a dislocation sink. During twin-slip interaction, at the location of impingement, the movements of the parent atoms may be interfered by the interaction, and this causes some parent atoms to shuffle to the faulted positions in the twin, leading to the widely observed PSFs inside the twin.

4.2. $\{10\bar{1}2\}$ TBs acting as dislocation sink as related to the twinning mechanism

From our simulation results, it appears that, when the Burgers vector of a matrix dislocation is parallel to the zone axis of the twins, the dislocation will be transmuted to a dislocation in the twin, and the two slip planes are simply the corresponding planes between the parent and the twin. Such a lattice correspondence can be well predicted by the classical twinning theory. However, when the Burgers vector of a matrix dislocation is not parallel to the zone axis of the twins, no dislocation transmutation occurs and the

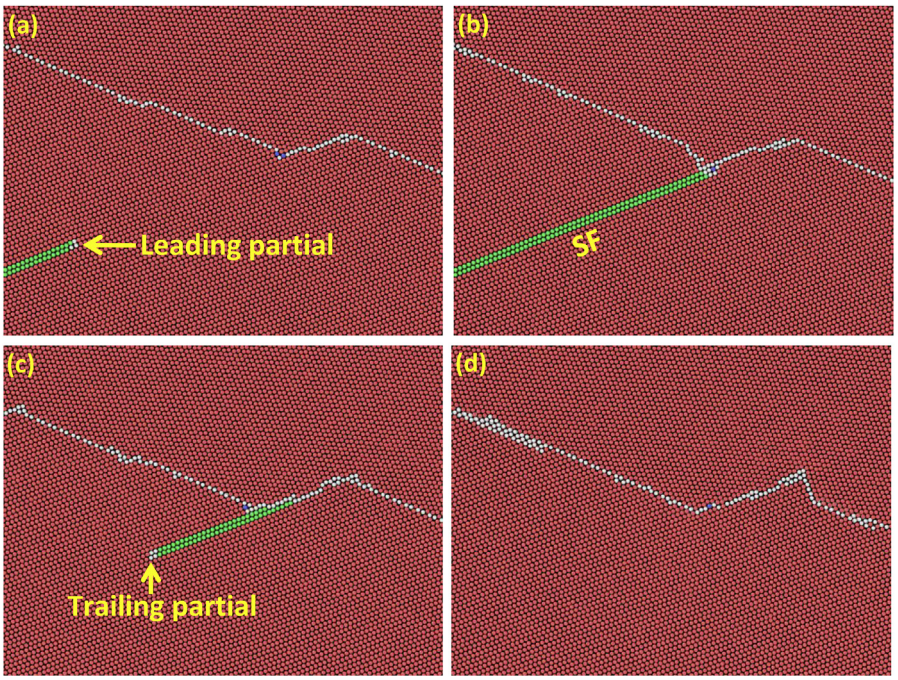

Fig. 12. Snapshots in time sequence showing the interaction between the mobile matrix basal dislocation and the mobile TB in the boxed region in Fig. 11. (a) The leading partial glides toward the TB. (b) The leading partial impinges on the TB. (c) The leading partial is absorbed by the TB while the trailing partial eliminating the SF and moving toward the TB. (d) All the partials and the SF are absorbed by the TB. No transmutation occurs.

dislocation will be absorbed by the TB. This important characteristic has not been reported before.

Another important factor is the coherence of a TB. It was reported that a matrix dislocation is able to transmit through a coherent twin boundary. Fang et al. [72] reported that in fcc metals, a screw dislocation in the parent will directly transmit into the twin when the TB is perfectly coherent; whereas a kinked, incoherent TB changes the interaction mechanism from dislocation transmission to dislocation absorption. They also suggested that the dislocation absorption mechanism does not contribute to hardening. Although dislocation transmission is different from dislocation transmutation, it appears that the coherence of a TB may strongly affect the interaction between matrix dislocations and the TB.

In experimental observations, most $\{10\bar{1}2\}\langle 10\bar{1}\bar{1}\rangle$ twin boundaries are extremely incoherent in the sense that they may hugely deviate from the $\{10\bar{1}2\}$ twinning plane [50–52], and the misorientation angle has a wide range of values unequal to the theoretical value of 86.3°. In atomistic simulations, $\left\{10\bar{1}2\right\}\left\langle 10\bar{1}\bar{1}\right\rangle$ twin boundaries are composed of coherent segments and incoherent basal/prismatic interfaces and the average TB are extremely incoherent as well [47,49,50]. Therefore, $\left\{10\bar{1}2\right\}\left\langle 10\bar{1}\bar{1}\right\rangle$ twin boundaries will act as a dislocation sink when matrix dislocations glide to the TBs, with the exception only for those dislocations that have a Burgers vector parallel to the zone axis of the twins.

Using atomistic simulations, Li and Ma [73] showed that $\{10\bar{1}2\}10\bar{1}1$ twinning is accomplished by the transformation of parent basal to twin prismatic and vice versa. This transformation only invokes atomic shuffling and no twinning dislocations are needed. This mechanism fundamentally differs from the classical twinning theory and the "disconnection model" [74,75]. Despite the difference, the Li-Ma model has been validated, though implicitly, by numerous researchers. Serra and Bacon [24] simulated the interaction between a screw dislocation and a $\{10\bar{1}2\}$ TB. They showed that a basal slip in the matrix was transformed to a prismatic slip in the twin, clearly indicating that the lattice transformation is "parent basal" to "twin prismatic" and vice versa, which is exactly the Li-Ma mechanism. Khater, Serra and Pond [76] analyzed the shearing and shuffling involved in $\{10\bar{1}2\}10\bar{1}1$ twinning by applying the classical twinning theory. It can be readily seen that their analysis ended up with exactly the "basal to prismatic" and "prismatic to basal" lattice transformation [77]. The shuffling mechanism can also readily be recognized in the simulations by Hirth et al. [78], Wang et al. [66], Barrett and El Kadiri [79]. In these works the misorientation angle equals 90°, thus the twinning shear must be zero and no twinning dislocation should be defined [50]. Recently, Gong et al. [26] simulated the interaction between basal dislocations and a $\{10\bar{1}2\}$ twin, transformation from a matrix basal dislocation to a twin prismatic dislocation was reported. Thus, the lattice transformation is exactly the same as the Li-Ma model as well [73]. Gong et al. [26] also reported that an $\langle a_2 \rangle$ basal dislocation was transformed to a $\frac{1}{2}\langle c+a \rangle$or $\langle c+a \rangle$. This transformation is mathematically possible but remains unclear because no Burgers vector analysis was conducted in their paper. Another interaction is also reported [80] in which a matrix dislocation dissociates at a TB forming twinning dislocations that cause the twin to grow or shrink, leaving behind a residual dislocation. This reaction is questionable because the twinning mechanism in these reports is actually the same as the shuffling mechanism [73], thus no twinning dislocation should exist. It can be readily shown [50] that during the transformation from parent basal to twin prismatic and vice versa, the $\{10\bar{1}2\}$ twinning plane must be distorted, thus the twinning plane is not an invariant plane and no homogeneous simple shear can occur on the twinning plane [77]. This is the very reason why $\{10\bar{1}2\}$ TBs are incoherent in most experimental observations and simulations.

The "twinning dislocation theories" for $\{10\bar{1}2\}$ mode were first questioned by Song and Gray [63,64]. In their TEM work, a high density of anomalous basal stacking faults, called "partial stacking faults", were observed. The presence of these PSFs cannot be

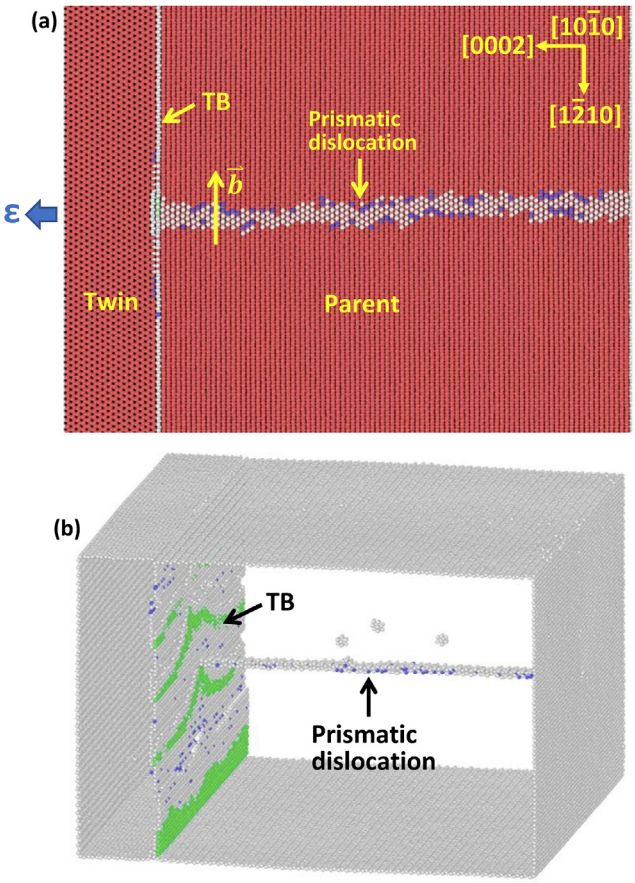

Fig. 13. (a) Initial configuration for simulating interaction between a matrix prismatic dislocation and a TB. The Burgers vector of the prismatic dislocation is parallel to the zone axis [1$\bar{2}$10] of the twins. The prismatic dislocation is slightly dissociated. A tensile load was applied along the [0002] of the parent. (b) 3D view of the TB and the prismatic dislocation. Atoms of hcp structure are removed.

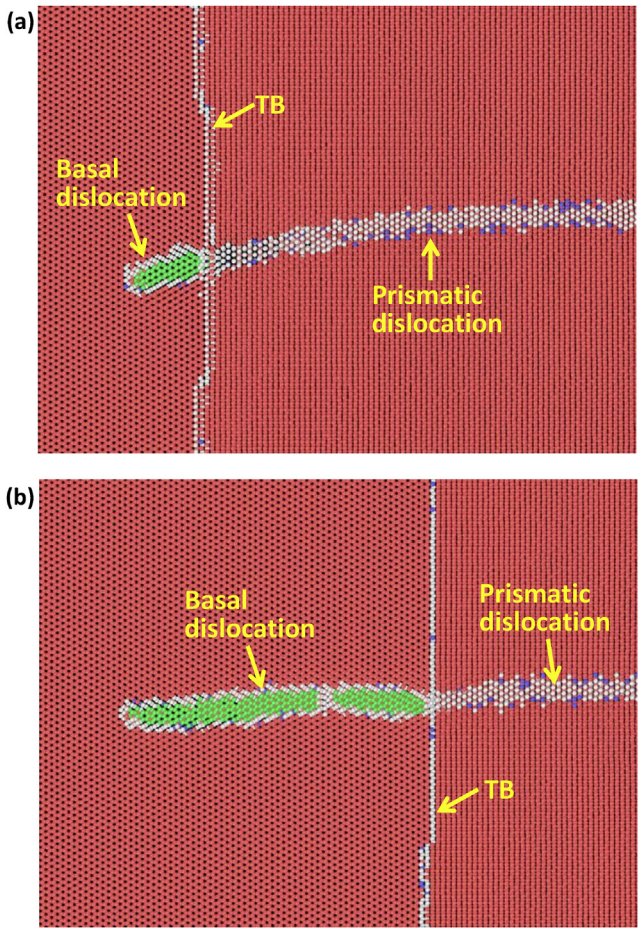

Fig. 14. (a) Under the tensile strain, the TB migrates and interacts with the prismatic dislocation. During interaction, the matrix prismatic dislocation is transformed to a basal dislocation in the twin. A basal SF (in green) bounded by two Shockley partials can be seen. (b) As the TB traverses through, the matrix prismatic dislocation is gradually transformed into a basal dislocation in the twin. (For interpretation of the references to color in this figure legend, the reader is referred to the Web version of this article.)

explained by the twinning dislocation theories. More recently, Cayron et al. [81] analytically proved that invariant plane strain condition, which is a fundamental condition in the classical twinning theory, does not hold for {10$\bar{1}$2} mode, calling into question the shearing paradigm for this particular twinning mode.

Dislocation absorption at {10$\bar{1}$2} TBs can be readily explained by the atomic shuffling mechanism [82]. Pan et al. [83] also reported that at the dislocation-grain boundaries impingement, the accommodation of free volume carried by incoming dislocations is associated with atomic shuffling. In our work, when the Burgers vectors of a matrix basal dislocation is parallel to the zone axis (Figs. 1–3), the incoming basal dislocation line can be transformed while the original Burgers vector is retained. The product dislocation is one of the real slip systems which is energetically favorable. Thus dislocation transmutation can occur. In contrast, when the Burgers vector of a matrix dislocation is not parallel to the zone axis, the original Burgers vector would be transformed to a corresponding vector in the twin, but such a product dislocation is likely energetically unfavorable and unstable. Thus, dislocation transmutation would not be feasible. As a result, the original dislocation line is "shredded" by atomic shuffling and absorbed by the TB. Presumably, if the Burgers vector of a product dislocation is very large, for example, $\langle c+a \rangle$, the core structure and its dissociation of such a dislocation could be very complex, transmutation would be unfavorable as well. This may explain why the prismatic dislocation with a Burgers vector non-parallel to the zone axis is still absorbed by the TB, even though the product dislocation is a possible slip system for hcp metals, i.e. $(\bar{1}2\bar{1}2)[\bar{1}2\bar{1}3]$, one of the $\langle c+a \rangle$ dislocations.

4.3. Correlation between dislocation sink and the hardening behavior

Twin-slip interaction has been considered as a hardening mechanism in deformation of Mg and Mg alloys on the basis that mobile dislocations in the matrix becomes immobile in the twin after transmutation at the TB [40,41,84–86]. This hardening mechanism was based on the Basinski effect [43] which was observed in fcc metals, as well as the dynamic Hall-Petch effect in which TBs were considered as extra grain boundaries that reduce the effective sizes of parent grains and a barrier to dislocation slip [85,87,88]. In the Basinski effect, glissile dislocations on the {111} planes were transformed to sessile dislocations on the {200} planes, resulting in strength/hardness increase in twin. In contrast to fcc metals, nano-indentation measurements in magnesium [45] show that the hardness difference between {10$\bar{1}$2} twin and matrix is insignificantly small, indicating the hardening by dislocation transmutation is ineffective in Mg. More recently, Chen et al. [46] reported that the contribution of {10$\bar{1}$2} twin-slip interaction to

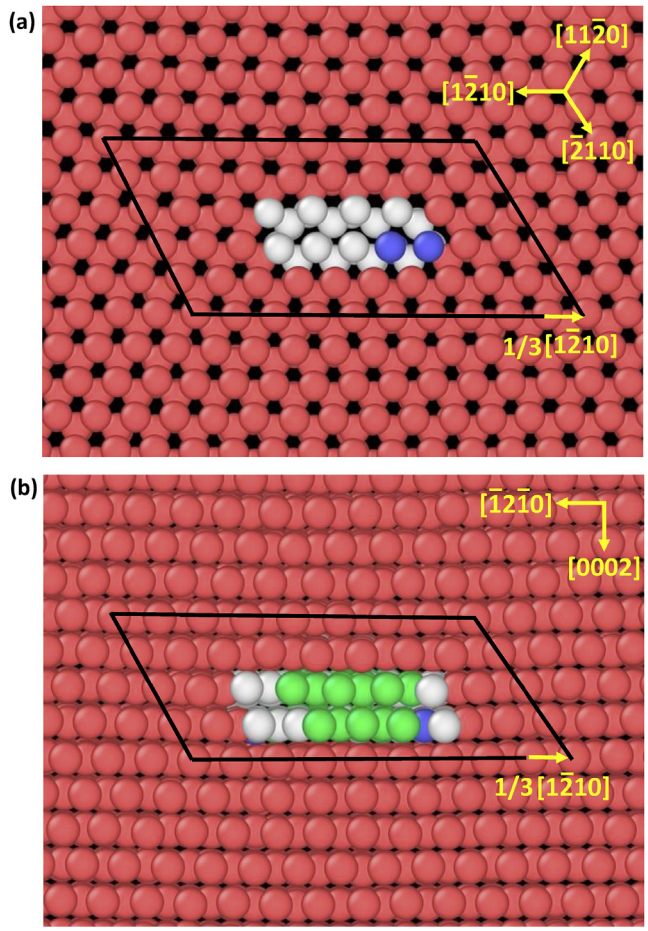

Fig. 15. Burgers vector analysis. (a) The Burgers vector of the matrix prismatic dislocation is identified as $\frac{1}{3}[\bar{1}2\bar{1}0]$. (b) The Burgers vector of the basal dislocation in the twin after the TB interacts and transforms the matrix prismatic dislocation. The Burgers vector remains parallel to the zone axis of the twins.

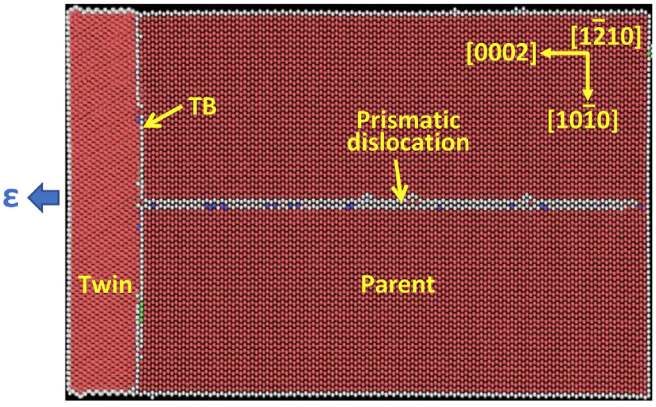

Fig. 16. Initial configuration for simulating interaction between a matrix prismatic dislocation and a TB while the Burgers vector of the prismatic dislocation makes 60° with the zone axis [1$\bar{2}$10] of the twins. A tensile load was applied along the [0002] of the parent.

hardening in an extruded AZ31 Mg alloy is negligible. In their work, specimens were pre-strained to 5% and 10% tensile strain such that only dislocation slip was activated. Then the specimens were subjected to compression such that $\{10\bar{1}2\}$ twinning was activated. Comparison of the stress-strain curves of these specimens shows

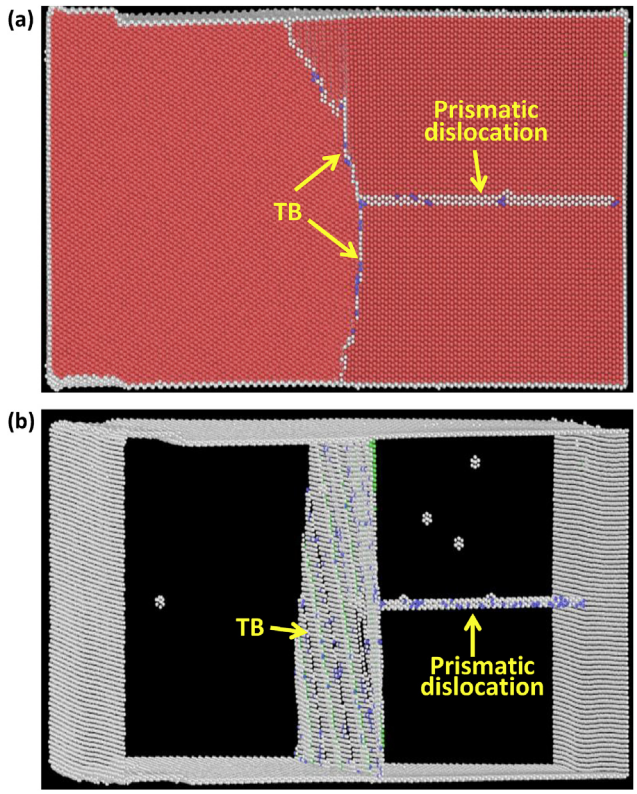

Fig. 17. (a) As the TB migrates into the parent and interacts with the matrix prismatic dislocation, the prismatic dislocation is being absorbed by the TB and no transmutation occurs. (b) 3D view showing the prismatic dislocation disappears after interacting with the TB.

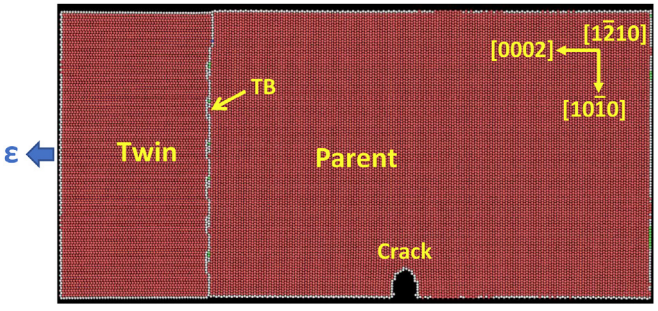

Fig. 18. Initial configuration for simulating the interaction between a TB and a $\{10\bar{1}1\}$ pyramidal dislocation. A nano-crack is pre-planted on the bottom surface of the parent to facilitate nucleation of pyramidal dislocations. A tensile load was applied along the [0002] of the parent.

negligible difference in the hardening behavior. Kalidindi et al. [34] also showed that the hardening effect of $\{10\bar{1}2\}$ twinning was very limited in Mg alloy. These reports indicate that twin-slip interaction may be not an important contributor to hardening for Mg and Mg alloys.

The hardening behavior in textured wrought Mg and Mg alloys can now be well correlated to our simulation results. At the early stage of plastic deformation, matrix dislocations especially the basal dislocations are activated. Immediately after the basal slip, $\{10\bar{1}2\}$ twinning is activated and twin growth dominates the deformation [20]. Based on our simulation results in this work, when the matrix dislocations interact with $\{10\bar{1}2\}$ TBs, most of them will likely be absorbed by the TBs that act as a dislocation

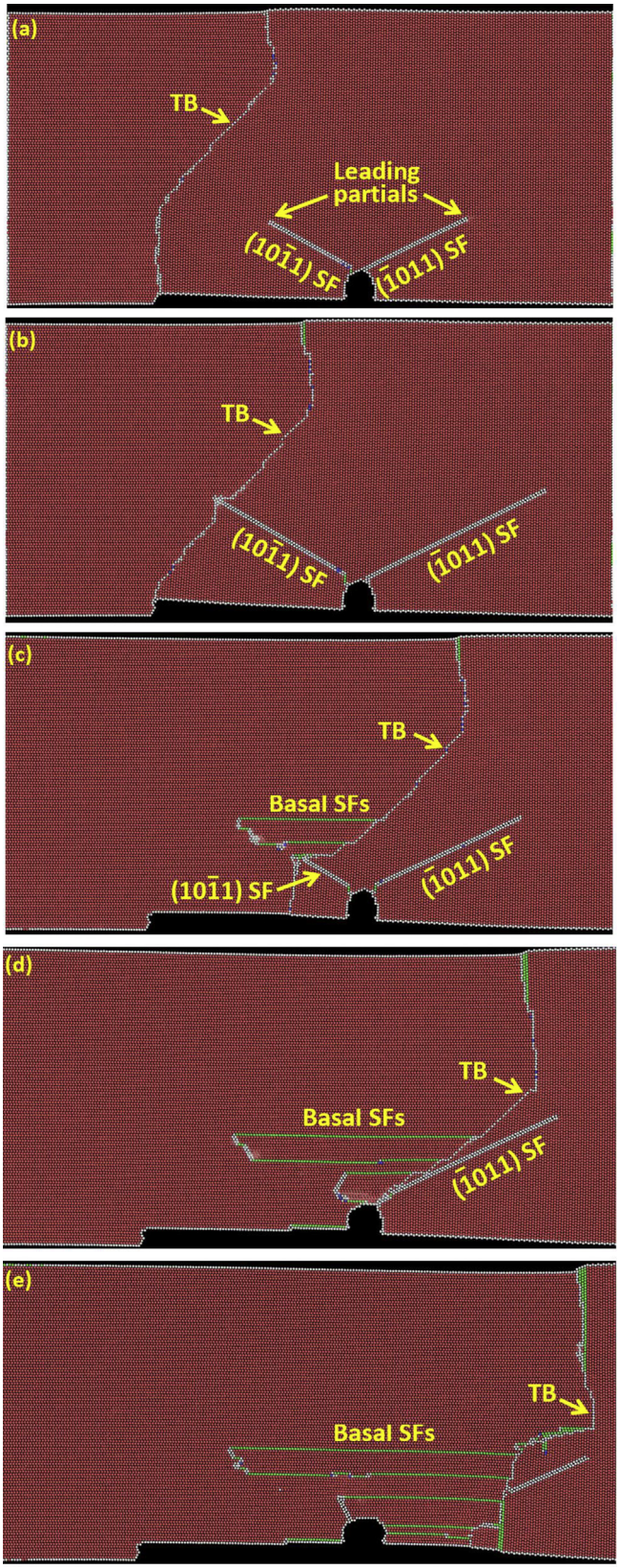

Fig. 19. Snapshots in time sequence showing the interaction between mobile matrix $\{10\bar{1}1\}$ pyramidal dislocations with a mobile TB. (a) Under the tensile loading, the TB starts migrating. Meanwhile, two $\{10\bar{1}1\}$ leading partials nucleate from the nano-crack, leaving SFs behind. (b) The left $\{10\bar{1}1\}$ leading partial impinges on the TB. (c) The leading partial is absorbed by the TB which continues migrating forward. At the location of impingement, a PSF is created. Along the wake of the leading partial, multiple PSFs are created as the TB interacts with the pyramidal SF. (d) The right ends of these PSFs are anchored at the TB and the SFs grow wider as the TB migrates. (e) The TB interacts with the other $\{10\bar{1}1\}$ pyramidal SF, erasing it and creating more PSFs inside the twin.

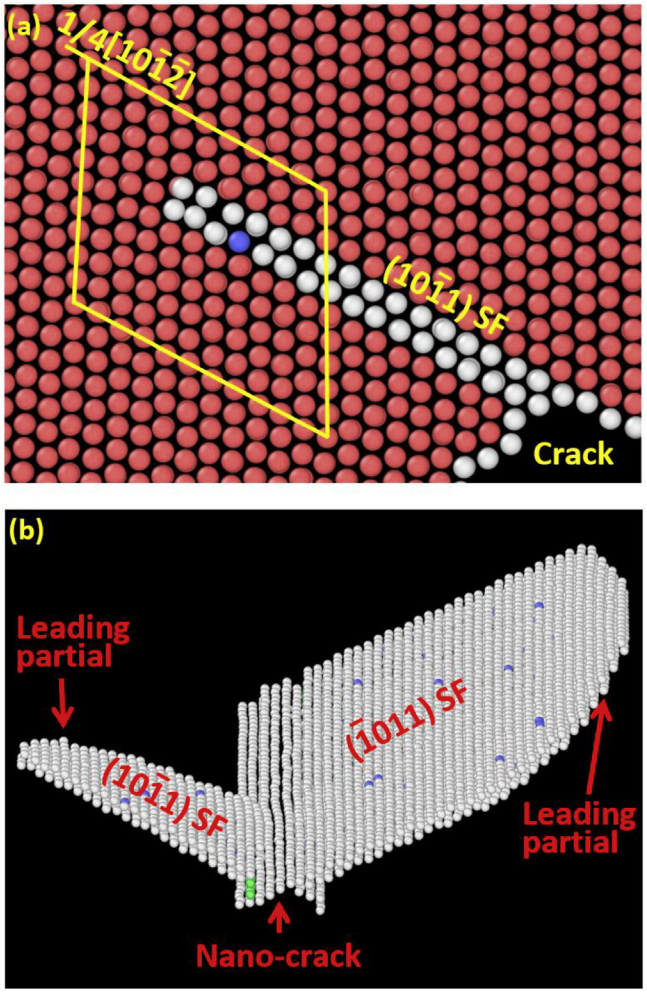

Fig. 20. Burgers vector analysis of the $\{10\bar{1}1\}$ pyramidal dislocations. (a) The Burgers vector of the leading partial is identified as $\frac{1}{4}[10\bar{1}2]$. (b) 3D view of the leading partials and the resultant SFs on the $(10\bar{1}1)$ and $(10\bar{1}1)$ planes.

sink, irrespective of dislocation types. Only those dislocations with Burgers vectors parallel to the zone axes of the twins can be transmuted. Consequently, the transmuted dislocations only account for a small portion of the matrix dislocations. As a result, the effect of twin-slip interaction on the hardening in Mg is insignificant. Also, during deformation the interaction energy barriers between the matrix dislocations and the TBs are only a few meV/atom, thus, the contribution of twin-slip interaction on hardening should be negligible.

5. Conclusions

In this work, interaction between a matrix dislocation and a $\{10\bar{1}2\}$ TB is systematically investigated by atomistic simulations. The following conclusions can be reached:

(1) When the Burgers vector of a matrix basal (prismatic) dislocation is parallel to the zone axis of the twins, the matrix basal (prismatic) dislocation can be transformed to a

Table 1
Dislocation transmutation [71] as compared to simulation results.

Parent slip system	Corresponding twin slip system	Simulation result
$(0001)[\bar{1}2\bar{1}0]$	$(10\bar{1}0)[\bar{1}2\bar{1}0]$	Observed
$(0001)[2\bar{1}\bar{1}0]$	$(\bar{1}010)[\bar{1}2\bar{1}3]$	Not observed
$(0001)[2\bar{1}\bar{1}0]$	$(\bar{1}010)[\bar{1}2\bar{1}3]$	Not observed
$(10\bar{1}0)[\bar{1}2\bar{1}0]$	$(000\bar{1})[1\bar{2}10]$	Observed
$(0\bar{1}10)[2\bar{1}\bar{1}0]$	$(\bar{1}2\bar{1}2)[\bar{1}2\bar{1}3]$	Not observed
$(\bar{1}100)[\bar{1}\bar{1}20]$	$(1\bar{2}\bar{1}2)[\bar{1}2\bar{1}3]$	Not observed

prismatic (basal) dislocation in the twin, with the original Burgers vector retained. This dislocation transmutation is consistent with the calculations based on the lattice correspondence in the classical twinning theory.

(2) When the Burgers vector of a matrix dislocation, irrespective of basal, prismatic and $\{10\bar{1}1\}$ pyramidal, is not parallel to the zone axis of the twins, the matrix dislocation is not transmuted. Instead, these dislocations are absorbed by the TB which acts as a dislocation sink.

(3) It appears that dislocation transmutation can only occur when the product dislocation in the twin is a real slip system, i.e. a slip system that is energetically favorable and stable. Otherwise dislocation transmutation cannot occur and the matrix dislocations will be absorbed by the TB.

(4) The twin-slip interaction revealed in our simulations can be well correlated to experimental observations which show twin-slip interaction only plays a very insignificant role in hardening in deformation of Mg and Mg alloys.

Acknowledgements

Bin Li gratefully thanks support from the U.S. National Science Foundation (NSF) (CMMI-1635088).

References

[1] S. Ni, Y.B. Wang, X.Z. Liao, R.B. Figueiredo, H.Q. Li, S.P. Ringer, T.G. Langdon, Y.T. Zhu, The effect of dislocation density on the interactions between dislocations and twin boundaries in nanocrystalline materials, Acta Mater. 60 (2012) 3181–3189, https://doi.org/10.1016/j.actamat.2012.02.026.
[2] H. Idrissi, D. Schryvers, Investigation of the Elementary Mechanisms Controlling Dislocation/twin Boundary Interactions in Fcc Metals and Alloys: from Conventional to Advanced TEM Characterization, 2012, p. 12.
[3] L. Rémy, Twin-slip interaction in f.c.c. crystals, Acta Metall. 25 (1977) 711–714, https://doi.org/10.1016/0001-6160(77)90013-X.
[4] L. Rémy, The interaction between slip and twinning systems and the influence of twinning on the mechanical behavior of fcc metals and alloys, Metall. Trans. A. 12 (1981) 387–408, https://doi.org/10.1007/BF02648536.
[5] Y.T. Zhu, X.L. Wu, X.Z. Liao, J. Narayan, L.J. Kecskés, S.N. Mathaudhu, Dislocation–twin interactions in nanocrystalline fcc metals, Acta Mater. 59 (2011) 812–821, https://doi.org/10.1016/j.actamat.2010.10.028.
[6] M.D. Sangid, T. Ezaz, H. Sehitoglu, Energetics of residual dislocations associated with slip–twin and slip–GBs interactions, Mater. Sci. Eng. 542 (2012) 21–30, https://doi.org/10.1016/j.msea.2012.02.023.
[7] B. Skrotzki, Crystallographic aspects of deformation twinning and consequences for plastic deformation processes in γ-TiAl, Acta Mater. 48 (2000) 851–862, https://doi.org/10.1016/S1359-6454(99)00385-7.
[8] Z.-H. Jin, P. Gumbsch, K. Albe, E. Ma, K. Lu, H. Gleiter, H. Hahn, Interactions between non-screw lattice dislocations and coherent twin boundaries in face-centered cubic metals, Acta Mater. 56 (2008) 1126–1135, https://doi.org/10.1016/j.actamat.2007.11.020.
[9] Z.X. Wu, Y.W. Zhang, D.J. Srolovitz, Dislocation–twin interaction mechanisms for ultrahigh strength and ductility in nanotwinned metals, Acta Mater. 57 (2009) 4508–4518, https://doi.org/10.1016/j.actamat.2009.06.015.
[10] M. Bönisch, Y. Wu, H. Sehitoglu, Hardening by slip-twin and twin-twin interactions in FeMnNiCoCr, Acta Mater. 153 (2018) 391–403, https://doi.org/10.1016/j.actamat.2018.04.054.
[11] T. Ezaz, M.D. Sangid, H. Sehitoglu, Energy barriers associated with slip–twin interactions, Philos. Mag. A 91 (2011) 1464–1488, https://doi.org/10.1080/14786435.2010.541166.
[12] T. Zhu, J. Li, A. Samanta, H.G. Kim, S. Suresh, Interfacial plasticity governs strain rate sensitivity and ductility in nanostructured metals, Proc. Natl. Acad. Sci. Unit. States Am. 104 (2007) 3031–3036, https://doi.org/10.1073/pnas.0611097104.
[13] X. Li, Y. Wei, L. Lu, K. Lu, H. Gao, Dislocation nucleation governed softening and maximum strength in nano-twinned metals, Nature 464 (2010) 877–880, https://doi.org/10.1038/nature08929.
[14] D. Jang, X. Li, H. Gao, J.R. Greer, Deformation mechanisms in nanotwinned metal nanopillars, Nat. Nanotechnol. 7 (2012) 594–601, https://doi.org/10.1038/nnano.2012.116.
[15] S.-W. Kim, X. Li, H. Gao, S. Kumar, In situ observations of crack arrest and bridging by nanoscale twins in copper thin films, Acta Mater. 60 (2012) 2959–2972, https://doi.org/10.1016/j.actamat.2012.02.002.
[16] Z. You, X. Li, L. Gui, Q. Lu, T. Zhu, H. Gao, L. Lu, Plastic anisotropy and associated deformation mechanisms in nanotwinned metals, Acta Mater. 61 (2013) 217–227, https://doi.org/10.1016/j.actamat.2012.09.052.
[17] J.W. Christian, S. Mahajan, Deformation twinning, Prog. Mater. Sci. 39 (1995) 1–157.
[18] M.H. Yoo, Slip, twinning, and fracture in hexagonal close-packed metals, Metall. Trans. A. 12 (1981) 409–418.
[19] E. Kelley, W. Hosford, Plane-strain compression of magnesium and magnesium alloy crystals, Trans Met Soc AIME 242 (1968) 5–13.
[20] P. Chen, B. Li, D. Culbertson, Y. Jiang, Contribution of extension twinning to plastic strain at low stress stage deformation of a Mg-3Al-1Zn alloy, Mater. Sci. Eng. 709 (2018) 40–45, https://doi.org/10.1016/j.msea.2017.10.038.
[21] S.-G. Hong, S.H. Park, C.S. Lee, Strain path dependence of {10–12} twinning activity in a polycrystalline magnesium alloy, Scripta Mater. 64 (2011) 145–148, https://doi.org/10.1016/j.scriptamat.2010.09.030.
[22] A.A. Luo, A.K. Sachdev, Development of a new wrought magnesium-aluminum-manganese alloy AM30, Metall. Mater. Trans. 38 (2007) 1184–1192, https://doi.org/10.1007/s11661-007-9129-2.
[23] P. Chen, F. Wang, J. Ombogo, B. Li, Formation of 60° ⟨01-10⟩ boundaries between {10-12} twin variants in deformation of a magnesium alloy, Mater. Sci. Eng. 739 (2019) 173–185, https://doi.org/10.1016/j.msea.2018.10.029.
[24] A. Serra, D.J. Bacon, Computer simulation of screw dislocation interactions with twin boundaries in H.C.P. metals, Acta Metall. Mater. 43 (1995) 4465–4481, https://doi.org/10.1016/0956-7151(95)00128-I.
[25] H. Fan, S. Aubry, A. Arsenlis, J.A. El-Awady, The role of twinning deformation on the hardening response of polycrystalline magnesium from discrete dislocation dynamics simulations, Acta Mater. 92 (2015) 126–139, https://doi.org/10.1016/j.actamat.2015.03.039.
[26] M. Gong, G. Liu, J. Wang, L. Capolungo, C.N. Tomé, Atomistic simulations of interaction between basal <a> dislocations and three-dimensional twins in magnesium, Acta Mater. 155 (2018) 187–198, https://doi.org/10.1016/j.actamat.2018.05.066.
[27] M.S. Hooshmand, M.J. Mills, M. Ghazisaeidi, Atomistic modeling of dislocation interactions with twin boundaries in Ti, Model. Simulat. Mater. Sci. Eng. 25 (2017), 045003, https://doi.org/10.1088/1361-651X/aa6323.
[28] A. Serra, D.J. Bacon, R.C. Pond, Dislocations in interfaces in the h.c.p. metals—I. Defects formed by absorption of crystal dislocations, Acta Mater. 47 (1999) 1425–1439, https://doi.org/10.1016/S1359-6454(99)00016-6.
[29] M. Yuasa, K. Masunaga, M. Mabuchi, Y. Chino, Interaction mechanisms of screw dislocations with and twin boundaries in Mg, Philos. Mag. A 94 (2014) 285–305, https://doi.org/10.1080/14786435.2013.853136.
[30] K.D. Molodov, T. Al-Samman, D.A. Molodov, Profuse slip transmission across twin boundaries in magnesium, Acta Mater. 124 (2017) 397–409, https://doi.org/10.1016/j.actamat.2016.11.022.
[31] T. Yoshida, M. Yuasa, M. Mabuchi, Y. Chino, Effect of segregated elements on the interactions between twin boundaries and screw dislocations in Mg, J. Appl. Phys. 118 (2015), 034304, https://doi.org/10.1063/1.4926947.
[32] Y. Xin, L. Lv, H. Chen, C. He, H. Yu, Q. Liu, Effect of dislocation-twin boundary interaction on deformation by twin boundary migration, Mater. Sci. Eng. 662 (2016) 95–99, https://doi.org/10.1016/j.msea.2016.03.061.
[33] B. Wang, R. Xin, G. Huang, Q. Liu, Effect of crystal orientation on the mechanical properties and strain hardening behavior of magnesium alloy AZ31 during uniaxial compression, Mater. Sci. Eng. 534 (2012) 588–593, https://doi.org/10.1016/j.msea.2011.12.013.
[34] M. Knezevic, A. Levinson, R. Harris, R.K. Mishra, R.D. Doherty, S.R. Kalidindi, Deformation twinning in AZ31: influence on strain hardening and texture evolution, Acta Mater. 58 (2010) 6230–6242, https://doi.org/10.1016/j.actamat.2010.07.041.
[35] S. r. Kalidindi, A. a. Salem, R. d. Doherty, Role of deformation twinning on strain hardening in cubic and hexagonal polycrystalline metals, Adv. Eng. Mater. 5 (2003) 229–232, https://doi.org/10.1002/adem.200300320.
[36] A. Serra, D.J. Bacon, R.C. Pond, Twins as barriers to basal slip in hexagonal-close-packed metals, Metall. Mater. Trans. 33 (2002) 809–812, https://doi.org/10.1007/s11661-002-0149-7.
[37] G. Proust, C.N. Tomé, A. Jain, S.R. Agnew, Modeling the effect of twinning and detwinning during strain-path changes of magnesium alloy AZ31, Int. J. Plast. 25 (2009) 861–880, https://doi.org/10.1016/j.ijplas.2008.05.005.
[38] A.A. Salem, S.R. Kalidindi, R.D. Doherty, Strain hardening of titanium: role of deformation twinning, Acta Mater. 51 (2003) 4225–4237, https://doi.org/10.1016/S1359-6454(03)00239-8.
[39] D. Culbertson, Q. Yu, J. Wang, Y. Jiang, Pre-compression effect on microstructure evolution of extruded pure polycrystalline magnesium during reversed tension load, Mater. Char. 134 (2017) 41–48, https://doi.org/10.1016/j.matchar.2017.10.003.

[40] H. El Kadiri, A.L. Oppedal, A crystal plasticity theory for latent hardening by glide twinning through dislocation transmutation and twin accommodation effects, J. Mech. Phys. Solid. 58 (2010) 613–624, https://doi.org/10.1016/j.jmps.2009.12.004.

[41] F. Wang, S.R. Agnew, Dislocation transmutation by tension twinning in magnesium alloy AZ31, Int. J. Plast. 81 (2016) 63–86, https://doi.org/10.1016/j.ijplas.2016.01.012.

[42] F. Wang, K. Hazeli, K.D. Molodov, C.D. Barrett, T. Al-Samman, D.A. Molodov, A. Kontsos, K.T. Ramesh, H. El Kadiri, S.R. Agnew, Characteristic dislocation substructure in {10-12} twins in hexagonal metals, Scripta Mater. 143 (2018) 81–85, https://doi.org/10.1016/j.scriptamat.2017.09.015.

[43] Z.S. Basinski, M.S. Szczerba, M. Niewczas, J.D. Embury, S.J. Basinski, The transformation of slip dislocations during twinning of copper-aluminum alloy crystals, Rev. Métall. 94 (1997) 1037–1044, https://doi.org/10.1051/metal/199794091037.

[44] L. Capolungo, I.J. Beyerlein, G.C. Kaschner, C.N. Tomé, On the interaction between slip dislocations and twins in HCP Zr, Mater. Sci. Eng. 513–514 (2009) 42–51, https://doi.org/10.1016/j.msea.2009.01.035.

[45] F. Hiura, R.K. Mishra, M. Lukitsch, M. Niewczas, Nano-indentation studies of twinned magnesium single crystals, in: Magnes. Technol. 2012, Springer, Cham, 2012, pp. 117–119, https://doi.org/10.1007/978-3-319-48203-3_22.

[46] P. Chen, B. Li, D. Culbertson, Y. Jiang, Negligible effect of twin-slip interaction on hardening in deformation of a Mg-3Al-1Zn alloy, Mater. Sci. Eng. 729 (2018) 285–293, https://doi.org/10.1016/j.msea.2018.05.067.

[47] B.-Y. Liu, J. Wang, B. Li, L. Lu, X.-Y. Zhang, Z.-W. Shan, J. Li, C.-L. Jia, J. Sun, E. Ma, Twinning-like lattice reorientation without a crystallographic twinning plane, Nat. Commun. 5 (2014), https://doi.org/10.1038/ncomms4297.

[48] B. Li, X.Y. Zhang, Global strain generated by shuffling-dominated {101-2}<10-1-1> twinning, Scripta Mater. 71 (2014) 45–48, https://doi.org/10.1016/j.scriptamat.2013.10.002.

[49] X.Y. Zhang, B. Li, Q. Liu, Non-equilibrium basal stacking faults in hexagonal close-packed metals, Acta Mater. 90 (2015) 140–150, https://doi.org/10.1016/j.actamat.2015.02.036.

[50] B. Li, X.Y. Zhang, Twinning with zero twinning shear, Scripta Mater. 125 (2016) 73–79, https://doi.org/10.1016/j.scriptamat.2016.07.004.

[51] X.Y. Zhang, B. Li, X.L. Wu, Y.T. Zhu, Q. Ma, Q. Liu, P.T. Wang, M.F. Horstemeyer, Twin boundaries showing very large deviations from the twinning plane, Scripta Mater. 67 (2012) 862–865, https://doi.org/10.1016/j.scriptamat.2012.08.012.

[52] X.Y. Zhang, B. Li, J. Tu, Q. Sun, Q. Liu, Non-classical twinning behavior in dynamically deformed cobalt, Mater. Res. Lett. 3 (2015) 142–148, https://doi.org/10.1080/21663831.2015.1034297.

[53] J.A. Yasi, T. Nogaret, D.R. Trinkle, Y. Qi, L.G.H. Jr, W.A. Curtin, Basal and prism dislocation cores in magnesium: comparison of first-principles and embedded-atom-potential methods predictions, Model. Simulat. Mater. Sci. Eng. 17 (2009), 055012, https://doi.org/10.1088/0965-0393/17/5/055012.

[54] M. Liao, B. Li, M.F. Horstemeyer, Interaction between prismatic slip and a Mg17Al12 precipitate in magnesium, Comput. Mater. Sci. 79 (2013) 534–539, https://doi.org/10.1016/j.commatsci.2013.07.016.

[55] B. Li, E. Ma, Pyramidal slip in magnesium: dislocations and stacking fault on the {1011} plane, Philos. Mag. A 89 (2009) 1223–1235, https://doi.org/10.1080/14786430902936707.

[56] H. Fan, J.A. El-Awady, Towards resolving the anonymity of pyramidal slip in magnesium, Mater. Sci. Eng. 644 (2015) 318–324, https://doi.org/10.1016/j.msea.2015.07.080.

[57] M.S. Daw, M.I. Baskes, Semiempirical, Quantum mechanical calculation of hydrogen embrittlement in metals, Phys. Rev. Lett. 50 (1983) 1285–1288, https://doi.org/10.1103/PhysRevLett.50.1285.

[58] M.S. Daw, M.I. Baskes, Embedded-atom method: derivation and application to impurities, surfaces, and other defects in metals, Phys. Rev. B 29 (1984) 6443–6453, https://doi.org/10.1103/PhysRevB.29.6443.

[59] X.-Y. Liu, J.B. Adams, F. Ercolessi, J.A. Moriarty, EAM potential for magnesium from quantum mechanical forces, Model. Simulat. Mater. Sci. Eng. 4 (1996) 293, https://doi.org/10.1088/0965-0393/4/3/004.

[60] B. Li, E. Ma, Zonal dislocations mediating {101-1}⟨10-1-2⟩ twinning in magnesium, Acta Mater. 57 (2009) 1734–1743, https://doi.org/10.1016/j.actamat.2008.12.016.

[61] A. Stukowski, Visualization and analysis of atomistic simulation data with OVITO–the Open Visualization Tool, Model. Simulat. Mater. Sci. Eng. 18 (2010), 015012, https://doi.org/10.1088/0965-0393/18/1/015012.

[62] J.D. Honeycutt, H.C. Andersen, Molecular dynamics study of melting and freezing of small Lennard-Jones clusters, J. Phys. Chem. 91 (1987) 4950–4963, https://doi.org/10.1021/j100303a014.

[63] S.G. Song, G.T. Gray, Structural interpretation of the nucleation and growth of deformation twins in Zr and Ti—I. Application of the coincidence site lattice (CSL) theory to twinning problems in h.c.p. structures, Acta Metall. Mater. 43 (1995) 2325–2337, https://doi.org/10.1016/0956-7151(94)00433-1.

[64] S.G. Song, G.T. Gray, Structural interpretation of the nucleation and growth of deformation twins in Zr and Ti—II. Tem study of twin morphology and defect reactions during twinning, Acta Metall. Mater. 43 (1995) 2339–2350, https://doi.org/10.1016/0956-7151(94)00434-X.

[65] A. Stukowski, V.V. Bulatov, A. Arsenlis, Automated identification and indexing of dislocations in crystal interfaces, Model. Simulat. Mater. Sci. Eng. 20 (2012), 085007, https://doi.org/10.1088/0965-0393/20/8/085007.

[66] J. Wang, S.K. Yadav, J.P. Hirth, C.N. Tomé, I.J. Beyerlein, Pure-shuffle nucleation of deformation twins in hexagonal-close-packed metals, Mater. Res. Lett. 1 (2013) 126–132, https://doi.org/10.1080/21663831.2013.792019.

[67] G. Henkelman, B.P. Uberuaga, H. Jónsson, A climbing image nudged elastic band method for finding saddle points and minimum energy paths, J. Chem. Phys. 113 (2000) 9901–9904, https://doi.org/10.1063/1.1329672.

[68] Z. Wu, W.A. Curtin, The origins of high hardening and low ductility in magnesium, Nature 526 (2015) 62–67, https://doi.org/10.1038/nature15364.

[69] Z. Wu, W.A. Curtin, Mechanism and energetics of ⟨c + a⟩ dislocation cross-slip in hcp metals, Proc. Natl. Acad. Sci. Unit. States Am. 113 (2016) 11137–11142, https://doi.org/10.1073/pnas.1603966113.

[70] J.W. Christian, The Theory of Transformations in Metals and Alloys, Newnes, 2002.

[71] M. Niewczas, Lattice correspondence during twinning in hexagonal close-packed crystals, Acta Mater. 58 (2010) 5848–5857, https://doi.org/10.1016/j.actamat.2010.06.059.

[72] Q. Fang, F. Sansoz, Influence of intrinsic kink-like defects on screw dislocation – coherent twin boundary interactions in copper, Acta Mater. 123 (2017) 383–393, https://doi.org/10.1016/j.actamat.2016.10.032.

[73] B. Li, E. Ma, Atomic shuffling dominated mechanism for deformation twinning in magnesium, Phys. Rev. Lett. 103 (2009), 035503, https://doi.org/10.1103/PhysRevLett.103.035503.

[74] A. Serra, D.J. Bacon, R.C. Pond, Comment on ``Atomic shuffling dominated mechanism for deformation twinning in magnesium'', Phys. Rev. Lett. 104 (2010), 029603 https://doi.org/10.1103/PhysRevLett.104.029603.

[75] B. Li, E. Ma, Li and Ma reply: Phys. Rev. Lett. 104 (2010), 029604 https://doi.org/10.1103/PhysRevLett.104.029604.

[76] H.A. Khater, A. Serra, R.C. Pond, Atomic shearing and shuffling accompanying the motion of twinning disconnections in zirconium, Philos. Mag. A 93 (2013) 1279–1298, https://doi.org/10.1080/14786435.2013.769071.

[77] X.Y. Zhang, B. Li, Q. Sun, On the {10-12} "twinning shear" measured from line deflection, Scripta Mater. 159 (2019) 133–136, https://doi.org/10.1016/j.scriptamat.2018.09.027.

[78] J.P. Hirth, J. Wang, C.N. Tomé, Disconnections and other defects associated with twin interfaces, Prog. Mater. Sci. 83 (2016) 417–471, https://doi.org/10.1016/j.pmatsci.2016.07.003.

[79] C.D. Barrett, H. El Kadiri, The roles of grain boundary dislocations and disclinations in the nucleation of {10-12} twinning, Acta Mater. 63 (2014) 1–15, https://doi.org/10.1016/j.actamat.2013.09.012.

[80] J. Wang, I.J. Beyerlein, C.N. Tomé, Reactions of lattice dislocations with grain boundaries in Mg: implications on the micro scale from atomic-scale calculations, Int. J. Plast. 56 (2014) 156–172, https://doi.org/10.1016/j.ijplas.2013.11.009.

[81] C. Cayron, R. Logé, Evidence of new twinning modes in magnesium questioning the shear paradigm, J. Appl. Crystallogr. 51 (2018) 809–817, https://doi.org/10.1107/S1600576718005678.

[82] A. Hasnaoui, P.M. Derlet, H. Van Swygenhoven, Interaction between dislocations and grain boundaries under an indenter – a molecular dynamics simulation, Acta Mater. 52 (2004) 2251–2258, https://doi.org/10.1016/j.actamat.2004.01.018.

[83] Z. Pan, T.J. Rupert, Damage nucleation from repeated dislocation absorption at a grain boundary, Comput. Mater. Sci. 93 (2014) 206–209, https://doi.org/10.1016/j.commatsci.2014.07.008.

[84] O. Muránsky, M.R. Barnett, V. Luzin, S. Vogel, On the correlation between deformation twinning and Lüders-like deformation in an extruded Mg alloy: in situ neutron diffraction and EPSC.4 modelling, Mater. Sci. Eng. 527 (2010) 1383–1394, https://doi.org/10.1016/j.msea.2009.10.018.

[85] G. Proust, C.N. Tomé, G.C. Kaschner, Modeling texture, twinning and hardening evolution during deformation of hexagonal materials, Acta Mater. 55 (2007) 2137–2148, https://doi.org/10.1016/j.actamat.2006.11.017.

[86] A.L. Oppedal, H. El Kadiri, C.N. Tomé, G.C. Kaschner, S.C. Vogel, J.C. Baird, M.F. Horstemeyer, Effect of dislocation transmutation on modeling hardening mechanisms by twinning in magnesium, Int. J. Plast. 30–31 (2012) 41–61, https://doi.org/10.1016/j.ijplas.2011.09.002.

[87] L. Jiang, J.J. Jonas, A.A. Luo, A.K. Sachdev, S. Godet, Influence of {10-12} extension twinning on the flow behavior of AZ31 Mg alloy, Mater. Sci. Eng. 445 (2007) 302–309, https://doi.org/10.1016/j.msea.2006.09.069.

[88] S.-G. Hong, S.H. Park, C.S. Lee, Role of {10–12} twinning characteristics in the deformation behavior of a polycrystalline magnesium alloy, Acta Mater. 58 (2010) 5873–5885, https://doi.org/10.1016/j.actamat.2010.07.002.